# Favre-Averaged Spatiotemporal-Filtered Large Eddy Simulation

Sean Walters*, Stephen Guzik†, and Xinfeng Gao‡

*Computational Fluid Dynamics and Propulsion Laboratory*

*Colorado State University, Fort Collins, CO 80523, USA*

**This study explores Favre-averaged space-time filtering of nonlinear partial differential equations for turbulence modeling. The mathematical derivation is presented in detail and the unknown terms resulting from the Favre-averaged space-time filtering process are provided. As a first step, this study focuses on identifying the mathematical operational difference between the proposed Favre-averaged spatial-temporal filtering and the traditional spatial-filtering processes, the resulting unknown terms, and potential issues in modeling these terms. Additionally, a rigorous nonlinear stability analysis is performed, helping identify advantages and disadvantages of each filtering approach.**

## I. Introduction

To model or simulate turbulent fluid flows, a mathematical model must first be developed and established for describing the fluid flow system at a certain level of approximation. Computational fluid dynamics (CFD) studies fluid systems numerically, where typically a range of temporal and spatial scales are present and nonlinear interactions exist among the physics occurring at different scales. The level of description and approximation in a broad sense will depend on the physical information that will be obtained from the model or simulation. In order to obtain the desired physical information, the scales directly associated with the physics of interest need to be resolved, and of course, the resolution will be subject to the reality of computing capability. In developing the mathematical model for turbulence modeling, two major operators are typically involved—filtering or averaging the original Navier-Stokes (NS) equations and closing the filtered or averaged NS equations. For example, two types of approximation commonly used in contemporary CFD modeling of turbulence, are the Reynolds-averaged Navier-Stokes (RANS)-based approach and the large eddy simulation (LES) approach. The RANS approach does not directly resolve the unsteady, turbulent fluid motions but instead resolves the time-averaged motions. The closure models employed by RANS are often based on physical intuition or experimental observations for canonical flow configurations and ad hoc hypotheses and assumptions are employed. Moreover, for RANS models designed to simulate flows with large scale, unsteady motions, a distinct spectral gap, as illustrated by Fig. 1, is necessary in the turbulent flow under consideration. RANS-based approaches in CFD modeling for turbulent flows have plateaued in their ability to resolve the critical technical challenges of the present.[1] LES of turbulent flows directly solves the large scales of turbulent fluid motions, while implicitly accounting for the small scales by using a sub-analytical-filter-scale (SFS) model. LES has been greatly developed since the 1960s and a review on LES research can be found in the reference.[2] The development of LES has also enabled its application not only in turbulent flow analysis but also in combustion, aero-acoustics and many other areas. This increased level of approximation in LES has shown great promise and demonstrated clear superiority over the RANS approach for moderately complex geometries. Although challenges and difficulties are still present in the SFS modeling and in wall modeling, it is promising that LES will find use in more complex engineering design situations than have been previously possible.[1]

It is, however, worth emphasizing that existing LES practice primarily employs spatially-filtered NS equations. While the time-filtering concept is an analog of space-filtering, explicit temporal-filtering of the

*Graduate Research Assistant, Email: walters2@rams.colostate.edu, Student Member AIAA

†Assistant Professor, Email: stephen.guzik@colostate.edu, Member AIAA

‡Associate Professor, Email: xinfeng.gao@colostate.edu, Member AIAA

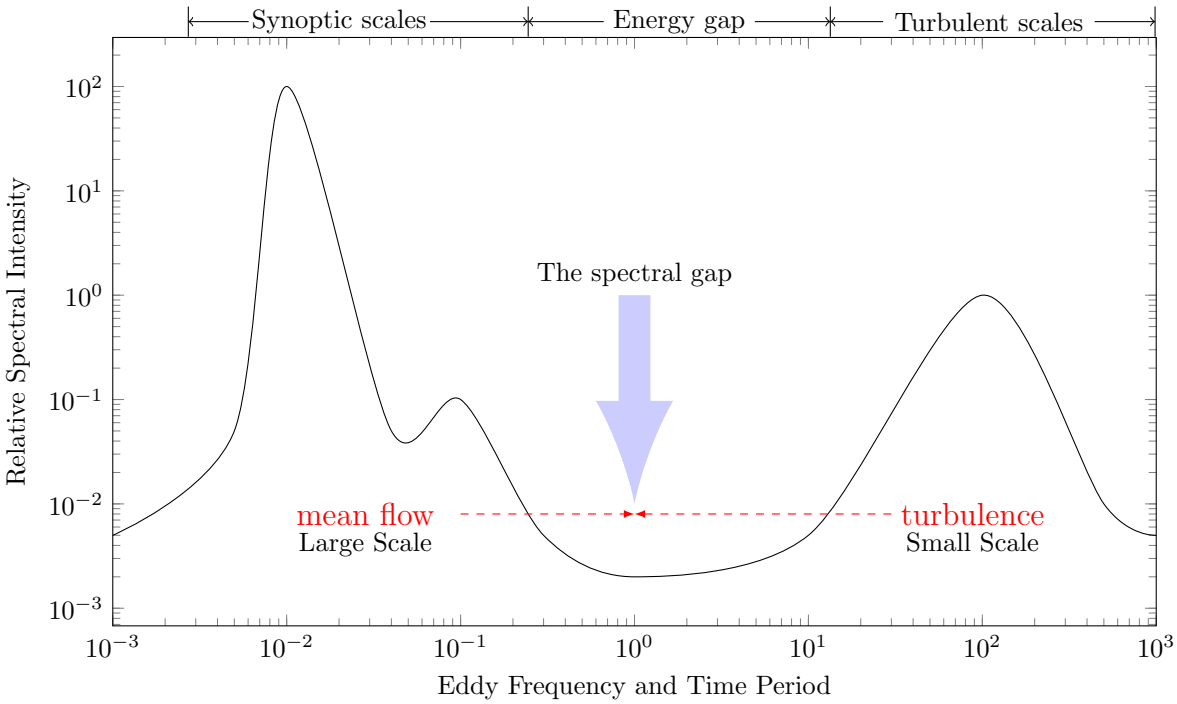


Figure 1: Illustration of spectral gap.

NS equations is rarely pursued. Although the discretization in time acts as an implicit filter in time, it is expected that explicit time-filtering can result in a better control of aliasing errors and the removal of unwanted spurious high-frequency solution contents. A few studies[3–6] considered the time-filtering concepts. For example, Dakhoul[3,4] first investigated the space-time filtering for the Burgers' equation; however no further investigations were carried out since 1986 in this regard. Work by Pruett[5] and Carati and Wray[6] involves a separate filtering process of time from space. In the present study, we explore an explicit, Favre-averaged, spatial-temporal-filtering approach for governing equations of compressible fluid flows.

The objectives of the present research are to

1. Establish the Favre-averaged space-time-filtering operators and rules.
2. Analyze the advantages and disadvantages of Favre-spatial-temporal-filtering approach from the mathematical, physical, and computational perspective. Favre-spatial-temporal filtering removes high wave number and high frequency components. In comparison to explicit spatial-filtering, will the Favre-spatial-temporal filtering
   - Curtail the importance attached to the ambiguous closure models?
   - Improve solution accuracy by removing or minimizing aliasing errors?
   - Increase computational efficiency in obtaining the solution?
3. Develop methods for assessing the solution quality and stability by applying space-time filtering to Burgers' equations.

The paper is structured as follows. First, the space-time filtering operators and the FAST operators are developed. Then, the mathematical details of the spatially-filtered and the spatial-temporal-filtered Burgers' equation are derived and presented for comparison. Furthermore, fourth-order discretization schemes are applied to the filtered equations resulting from both filtering methods, and the numerical stability associated with each filtering method is analyzed. Finally, the numerical solutions are presented, compared, and discussed. Future follow-up investigations are suggested.

## II. Notations and Definitions

This section introduces the notation and definitions used in the Favre-averaged space-time LES approach, also referred to as FAST LES in this study. Applying a space and time filter on a random field $\phi(\vec{x},t)$, we get a spatially and temporally filtered random field. The filtered field is defined as:[7]

$$\bar{\phi}(\vec{x},t) = \int_{-\infty}^{\infty}\int_{-\infty}^{\infty} \phi(\vec{\xi},\tau)G(\vec{x}-\vec{\xi},t-\tau)d\tau d\vec{\xi}\,, \tag{1}$$

where $G$ is the filter convolution kernel function which has the cut off length $\Delta_{\vec{x}}$ and cut off time $\Delta_\tau$. Smaller motions will not be resolved and should be modeled. In general, we can express $\phi$ as

$$\phi(\vec{x},t) = \overline{\phi}(\vec{x},t) + \phi'(\vec{x},t)\,, \tag{2}$$

where $\overline{\phi}(\vec{x},t)$ represents the component resolved by a filter and $\phi'(\vec{x},y)$ represents the component which is unresolvable by a filter. For example, the grid used to discretize the equations is a filter, only resolving components down to a specific resolution and leaving smaller features unresolved. By the definition of Eq. (1), the filtered density, $\bar{\rho}$, is

$$\bar{\rho}(\vec{x},t) = \int_{-\infty}^{\infty}\int_{-\infty}^{\infty} \rho(\vec{\xi},\tau)G(\vec{x}-\vec{\xi},t-\tau)d\tau d\vec{\xi}. \tag{3}$$

For compressible flows, we introduce a Favre-averaged filtered velocity, $\tilde{u}$, as

$$\tilde{u}(\vec{x},t) = \frac{\int_{-\infty}^{\infty}\int_{-\infty}^{\infty} \rho u(\vec{\xi},\tau)G(\vec{x}-\vec{\xi},t-\tau)d\tau d\vec{\xi}}{\bar{\rho}(\vec{x},t)}\,. \tag{4}$$

For the Favre-averaged filtered velocity, using Eq. (4), the filtering of $\rho u$ and $\rho uu$ are defined to be

$$\overline{\rho u}(\vec{x},t) = \int_{-\infty}^{\infty}\int_{-\infty}^{\infty} \rho u(\vec{\xi},\tau)G(\vec{x}-\vec{\xi},t-\tau)d\tau d\vec{\xi} = \overline{\rho}\tilde{u}(\vec{x},t)\,, \tag{5}$$

and

$$\overline{\rho uu}(\vec{x},t) = \int_{-\infty}^{\infty}\int_{-\infty}^{\infty} \rho uu(\vec{\xi},\tau)G(\vec{x}-\vec{\xi},t-\tau)d\tau d\vec{\xi} = \overline{\rho}\widetilde{uu}(\vec{x},t)\,. \tag{6}$$

Note that in the present study, we use the following terminology interchangeably: Favre-spatiotemporal-filtering, Favre-averaged spatiotemporal-filtering, Favre-averaged space-time-filtering, Favre-averaged spatiotemporal-filtered, Favre-averaged space-time filtering. All of the preceding terminology is acronymed FAST.

## III. Space-Time Filtering Operators

### III.A. Filter Function and Filter Size

The choice of explicit filter function and filter size in the development of FAST-LES equations is critical in terms of the control of discretization errors in both space and time. The Gaussian filter[3,7] demonstrates superior properties to the box filter in filtering out the high frequency and high wave number components. For clarity, we use the Gaussian filter in the derivation and analysis of FAST LES in the present study.

Following Dakhoul,[3] the Gaussian filter can be written as

$$G(\vec{x},t) = G(t)\prod_{d=1}^{D} G_d(\vec{x})\,, \tag{7}$$

where $D$ is the number of spatial dimensions, $d$ is the index of spatial dimensions, and $G(t)$ and $G_d(\vec{x})$ are the temporal and spatial components, respectively, given by

$$G(t) = \sqrt{\frac{\gamma}{\pi}}\frac{1}{\Delta_\tau}e^{(-\gamma t^2/\Delta_\tau^2)} \tag{8}$$

$$G_d(\vec{x}) = \sqrt{\frac{\gamma}{\pi}}\frac{1}{\Delta_d}e^{(-\gamma x_d^2/\Delta_d^2)}\,. \tag{9}$$

In the equation, $\gamma$ is the filter constant, $\Delta_\tau$ the temporal filter width, and $\Delta_d$ is the spatial filter width in the $d$-direction in space. The explicit filter width for $\Delta_{\vec{x}}$ and $\Delta_\tau$ is chosen to be at least twice the spatial and temporal resolution, respectively.

### III.B. Filter Rules: Exact

The following rules of the convolution filtering operator are applied, and they are:

$$\overline{\phi_1 + \phi_2 + ...} = \overline{\phi_1} + \overline{\phi_2} + ... \tag{10}$$

$$\overline{\frac{\partial \phi}{\partial t}} = \int_{-\infty}^{\infty} \frac{\partial \phi(\vec{\xi}, \tau)}{\partial \tau} G(\vec{x} - \vec{\xi}, t - \tau) d\vec{\xi} d\tau = \frac{\partial \overline{\phi}}{\partial t} \tag{11}$$

$$\overline{\frac{\partial \phi}{\partial x_i}} = \frac{\partial \overline{\phi}}{\partial x_i} \tag{12}$$

$$\overline{\overline{\phi}_i \overline{\phi}_j}(\vec{x}, t) = \int_{-\infty}^{\infty} G(\vec{x} - \vec{\xi}, t - \tau) \overline{\phi}_i \overline{\phi}_j(\vec{\xi}, \tau) d\vec{\xi} d\tau \tag{13}$$

### III.C. Filter Rules: Approximations

In Eq. (13), the term $\overline{\phi}_i \overline{\phi}_j(\vec{\xi}, \tau)$ can be further expanded by using a Taylor expansion at the reference state $(\vec{x}, t)$ as

$$\begin{aligned}
\overline{\phi}_i \overline{\phi}_j(\vec{\xi}, \tau) &= \overline{\phi}_i \overline{\phi}_j \Big( \vec{x} + (\vec{\xi} - \vec{x}), t + (\tau - t) \Big) \\
&= \overline{\phi}_i \overline{\phi}_j(\vec{x}, t) + (\tau - t) \frac{\partial (\overline{\phi}_i \overline{\phi}_j(\vec{x}, t))}{\partial t} + \sum_{d=1}^{D} (\vec{\xi} - \vec{x}) \frac{\partial (\overline{\phi}_i \overline{\phi}_j(\vec{x}, t))}{\partial x_d} \\
&+ \frac{1}{2} (\tau - t)^2 \frac{\partial^2 (\overline{\phi}_i \overline{\phi}_j(\vec{x}, t))}{\partial t^2} + \frac{1}{2} \sum_{d,e=1}^{D} (\xi_d - x_d)(\xi_e - x_e) \frac{\partial^2 (\overline{\phi}_i \overline{\phi}_j(\vec{x}, t))}{\partial x_d \partial x_e} \\
&+ \sum_{d=1}^{D} (\xi_d - x_d)(\tau - t) \frac{\partial^2 (\overline{\phi}_i \overline{\phi}_j(\vec{x}, t))}{\partial x_d \partial t} + \frac{1}{2} \sum_{d=1}^{D} (\vec{\xi} - \vec{x})^2 \frac{\partial^2 (\overline{\phi}_i \overline{\phi}_j(\vec{x}, t))}{\partial x_d^2} + \text{H.O.T.}
\end{aligned} \tag{14}$$

Substituting the above expansion into Eq. (13) and neglecting the high order terms (H.O.T.), we arrive at

$$\begin{aligned}
\overline{\overline{\phi}_i \overline{\phi}_j} &= \overline{\phi}_i \overline{\phi}_j \int_{-\infty}^{\infty} G(\vec{x} - \vec{\xi}, t - \tau) d\vec{\xi} d\tau + \frac{\partial (\overline{\phi}_i \overline{\phi}_j)}{\partial t} \int_{-\infty}^{\infty} (\tau - t) G(\vec{x} - \vec{\xi}, t - \tau) d\vec{\xi} d\tau \\
&+ \sum_{d=1}^{D} \frac{\partial (\overline{\phi}_i \overline{\phi}_j)}{\partial x_d} \int_{-\infty}^{\infty} (\vec{\xi}_d - x_d) G(\vec{x} - \vec{\xi}, t - \tau) d\vec{\xi} d\tau + \frac{1}{2} \frac{\partial^2 (\overline{\phi}_i \overline{\phi}_j)}{\partial t^2} \int_{-\infty}^{\infty} (\tau - t)^2 G(\vec{x} - \vec{\xi}, t - \tau) d\vec{\xi} d\tau \\
&+ \frac{1}{2} \sum_{d=1}^{D} \frac{\partial^2 (\overline{\phi}_i \overline{\phi}_j)}{\partial x_d^2} \int_{-\infty}^{\infty} (\xi_d - x_d)^2 G(\vec{x} - \vec{\xi}, t - \tau) d\vec{\xi} d\tau \\
&+ \frac{1}{2} \sum_{d,e=1}^{D} \frac{\partial^2 (\overline{\phi}_i \overline{\phi}_j(\vec{x}, t))}{\partial x_d \partial x_e} \int_{-\infty}^{\infty} (\xi_d - x_d)(\xi_e - x_e) G(\vec{x} - \vec{\xi}, t - \tau) d\vec{\xi} d\tau \\
&+ \sum_{d=1}^{D} \frac{\partial^2 (\overline{\phi}_i \overline{\phi}_j(\vec{x}, t))}{\partial x_d \partial t} \int_{-\infty}^{\infty} (\xi_d - x_d)(\tau - t) G(\vec{x} - \vec{\xi}, t - \tau) d\vec{\xi} d\tau \,.
\end{aligned} \tag{15}$$

A helpful property arises when the Gaussian filter is applied to the Taylor expansion of $\phi_i$. All of the expansion terms containing odd-order derivatives (including mixed derivatives that contain at least one odd-order) will evaluate to zero when integrated over the specified interval. Therefore, for the Gaussian filter kernel, the above equation can be simplified as

$$\overline{\overline{\phi}_i \overline{\phi}_j} = \overline{\phi}_i \overline{\phi}_j + \frac{\Delta_\tau^2}{4\gamma} \frac{\partial^2 \overline{\phi}_i \overline{\phi}_j}{\partial t^2} + \sum_{d=1}^{D} \left( \frac{\Delta_d^2}{4\gamma} \right) \frac{\partial^2 \overline{\phi}_i \overline{\phi}_j}{\partial x_d^2} \,. \tag{16}$$

This relation will be used in the development of modeling the unknown terms resulting from the filtering process for our applications. However, Eq. (13), or the term $\overline{\overline{\phi}_i\overline{\phi}_j}$, can be obtained by a using a different methodology. This methodology and some mathematical details are provided in Appendix A.

### III.D. A Condensed Form of the Nonlinear Term

The goal of this section is to determine an easily expressible, condensed form of the entire filtered nonlinear term, $\overline{\phi_i\phi_j}$. First, it is noted that a decomposition of the nonlinear term can be expressed as

$$\phi_i\phi_j = \overline{\phi}_i\overline{\phi}_j + \overline{\phi}_i\phi'_j + \phi'_i\overline{\phi_j} + \phi'_i\phi'_j \ , \tag{17}$$

and a decomposition of the filtered nonlinear term can be expressed as

$$\overline{\phi_i\phi_j} = \overline{\overline{\phi}_i\overline{\phi}_j} + \overline{\overline{\phi}_i\phi'_j} + \overline{\phi'_i\overline{\phi_j}} + \overline{\phi'_i\phi'_j} \ . \tag{18}$$

Equation (17) can be rearranged as

$$\overline{\phi}_i\overline{\phi}_j(\vec{x},t) - \phi_i\phi_j(\vec{x},t) = -\overline{\phi}_i\phi'_j(\vec{x},t) - \phi'_i\overline{\phi}_j(\vec{x},t) - \phi'_i\phi'_j(\vec{x},t) \ . \tag{19}$$

The right hand side of Eq. (19) can be written in a more instructive form using Eq. (71) as

$$\begin{aligned}\overline{\phi}_i\phi'_j(\vec{x},t) + \phi'_i\overline{\phi}_j(\vec{x},t) + \phi'_i\phi'_j(\vec{x},t) = &-\frac{\Delta_\tau^2}{4\gamma}\phi_i(\vec{x},t)\frac{\partial^2\phi_j(\vec{x},t)}{\partial t^2} - \sum_{d=1}^{D}\frac{\Delta_d^2}{4\gamma}\phi_i(\vec{x},t)\frac{\partial^2\phi_j(\vec{x},t)}{\partial x_d^2} \\ &- \frac{\Delta_\tau^2}{4\gamma}\phi_j(\vec{x},t)\frac{\partial^2\phi_i(\vec{x},t)}{\partial t^2} - \sum_{d=1}^{D}\frac{\Delta_d^2}{4\gamma}\phi_j(\vec{x},t)\frac{\partial^2\phi_i(\vec{x},t)}{\partial x_d^2} + \text{H.O.T.}\end{aligned} \tag{20}$$

The next step of the process is to filter just $\phi_i\phi_j$ as Eq. (68). Doing so leads to the form

$$\begin{aligned}\overline{\phi_i\phi_j} &= \int_{-\infty}^{\infty} G(\vec{x}-\vec{\xi},t-\tau)\phi_i\phi_j(\vec{\xi},\tau) \\ &= \phi_i\phi_j + \frac{\Delta_\tau^2}{4\gamma}\frac{\partial^2\phi_i\phi_j}{\partial t^2} + \sum_{d=1}^{D}\left(\frac{\Delta_d^2}{4\gamma}\right)\frac{\partial^2\phi_i\phi_j}{\partial x_d^2} + \text{H.O.T.}\end{aligned} \tag{21}$$

which can be further expressed by substituting Eq. (17) into $\phi_i\phi_j$ as

$$\begin{aligned}\overline{\phi_i\phi_j} = &\ \overline{\phi}_i\overline{\phi}_j(\vec{x},t) + \overline{\phi}_i\phi'_j(\vec{x},t) + \phi'_i\overline{\phi}_j(\vec{x},t) + \phi'_i\phi'_j(\vec{x},t) \\ &+ \frac{\Delta_\tau^2}{4\gamma}\phi_i(\vec{x},t)\frac{\partial^2\phi_j(\vec{x},t)}{\partial t^2} + \sum_{d=1}^{D}\frac{\Delta_d^2}{4\gamma}\phi_i(\vec{x},t)\frac{\partial^2\phi_j(\vec{x},t)}{\partial x_d^2} \\ &+ \frac{\Delta_\tau^2}{4\gamma}\phi_j(\vec{x},t)\frac{\partial^2\phi_i(\vec{x},t)}{\partial t^2} + \sum_{d=1}^{D}\frac{\Delta_d^2}{4\gamma}\phi_j(\vec{x},t)\frac{\partial^2\phi_i(\vec{x},t)}{\partial x_d^2} \\ &+ \frac{\Delta_\tau^2}{2\gamma}\left(\frac{\partial\phi_i(\vec{x},t)}{\partial t}\right)\left(\frac{\partial\phi_j(\vec{x},t)}{\partial t}\right) + \sum_{d=1}^{D}\frac{\Delta_d^2}{2\gamma}\left(\frac{\partial\phi_i(\vec{x},t)}{\partial x_d}\right)\left(\frac{\partial\phi_j(\vec{x},t)}{\partial x_d}\right) + \text{H.O.T.}\end{aligned} \tag{22}$$

Substituting Eq. (20) into Eq. (22) provides a condensed form of the nonlinear term given as

$$\overline{\phi_i\phi_j} = \overline{\phi}_i\overline{\phi}_j + \frac{\Delta_\tau^2}{2\gamma}\left(\frac{\partial\phi_i(\vec{x},t)}{\partial t}\right)\left(\frac{\partial\phi_j(\vec{x},t)}{\partial t}\right) + \sum_{d=1}^{D}\frac{\Delta_d^2}{2\gamma}\left(\frac{\partial\phi_i(\vec{x},t)}{\partial x_d}\right)\left(\frac{\partial\phi_j(\vec{x},t)}{\partial x_d}\right) + \text{H.O.T.} \tag{23}$$

This condensed form greatly simplifies the number of terms necessary to approximate the nonlinear term numerically. Formulations of the nonlinear term presented further on in this paper treat each of the three components of the nonlinear term separately in order to determine what effects each may have on the computational efficiency and accuracy and how the individual terms may be approximated in the compact formulation. Although this is the case, no assumptions aside from differentiability have been applied in order to derive this result. Therefore, this derivation is considered more complete (but potentially less instructive) than any of the other derivations of the nonlinear term presented in this paper.

## IV. Favre-Averaged Space-Time Filtering Operators

For LES of compressible flows, a change-of-variable is typically introduced in order that the nonlinear interaction of the density and the velocity within the continuity equation will not produce a term that requires modeling. This change-of-variable is the Favre-averaging presented in Eq. (4). Accordingly, the operator of $\widetilde{u_i u_j}$ can be evaluated by

$$\widetilde{u_i u_j} = \widetilde{\tilde{u}_i \tilde{u}_j} + \widetilde{\tilde{u}_i u'_j} + \widetilde{u'_i \tilde{u}_j} + \widetilde{u'_i u'_j}. \tag{24}$$

For the first term on the right, we can express it according to Eq. (16) as

$$\widetilde{\tilde{u}_i \tilde{u}_j} = \tilde{u}_i \tilde{u}_j + \left(\frac{\Delta_t^2}{4\gamma}\right)\frac{\partial^2 \tilde{u}_i \tilde{u}_j}{\partial t^2} + \sum_{d=1}^{D}\left(\frac{\Delta_d^2}{4\gamma}\right)\frac{\partial^2 \tilde{u}_i \tilde{u}_j}{\partial x_d^2}. \tag{25}$$

The approximation of the second and third terms on the right of Eq. (24) will be derived next.

### IV.A. Approximation of Turbulent Transport Terms, $\widetilde{\tilde{u}u'}$

It is known that all of the terms in Eq. (24) that include the $u'$ term must be modeled or approximated. First, by analog to Eq. (68) for reducing the order of the filter terms,[8] we obtain the following formula for each velocity component,

$$\begin{aligned}
\tilde{u}_i &= u_i + \left(\frac{\Delta_t^2}{4\gamma}\right)\frac{\partial^2 u_i}{\partial t^2} + \sum_{d=1}^{D}\left(\frac{\Delta_d^2}{4\gamma}\right)\frac{\partial^2 u_i}{\partial x_d^2}\,, \\
u'_i &= u_i - \tilde{u}_i \\
&= -\left(\frac{\Delta_t^2}{4\gamma}\right)\frac{\partial^2 u_i}{\partial t^2} - \sum_{d=1}^{D}\left(\frac{\Delta_d^2}{4\gamma}\right)\frac{\partial^2 u_i}{\partial x_d^2}\,, \\
&= -\left(\frac{\Delta_t^2}{4\gamma}\right)\frac{\partial^2 (\tilde{u}_i + u'_i)}{\partial t^2} - \sum_{d=1}^{D}\left(\frac{\Delta_d^2}{4\gamma}\right)\frac{\partial^2 (\tilde{u}_i + u'_i)}{\partial x_d^2}\,.
\end{aligned} \tag{26}$$

Multiplying both sides by $\tilde{u}_i$ yields:

$$\tilde{u}_i u'_j = -\left(\frac{\Delta_t^2}{4\gamma}\right)\left\{\tilde{u}_i \frac{\partial^2 \tilde{u}_j}{\partial t^2} + \tilde{u}_i \frac{\partial^2 u'_j}{\partial t^2}\right\} - \sum_{d=1}^{D}\left(\frac{\Delta_d^2}{4\gamma}\right)\left\{\tilde{u}_i \frac{\partial^2 \tilde{u}_j}{\partial x_d^2} + \tilde{u}_i \frac{\partial^2 u'_j}{\partial x_d^2}\right\}. \tag{27}$$

Applying the filtering rules (Eqs. 10-12) to the equation above yields:

$$\widetilde{\tilde{u}_i u'_j} = -\left(\frac{\Delta_t^2}{4\gamma}\right)\left\{\widetilde{\tilde{u}_i \frac{\partial^2 \tilde{u}_j}{\partial t^2}} + \widetilde{\tilde{u}_i \frac{\partial^2 u'_j}{\partial t^2}}\right\} - \sum_{d=1}^{D}\left(\frac{\Delta_d^2}{4\gamma}\right)\left\{\widetilde{\tilde{u}_i \frac{\partial^2 \tilde{u}_j}{\partial x_d^2}} + \widetilde{\tilde{u}_i \frac{\partial^2 u'_j}{\partial x_d^2}}\right\}. \tag{28}$$

Assuming the fluctuation is of an order of magnitude smaller than the filtered value, we neglect the second derivative of the fluctuations to arrive at

$$\widetilde{\tilde{u}_i u'_j} = -\left(\frac{\Delta_t^2}{4\gamma}\right)\widetilde{\tilde{u}_i \frac{\partial^2 \tilde{u}_j}{\partial t^2}} - \sum_{d=1}^{D}\left(\frac{\Delta_d^2}{4\gamma}\right)\widetilde{\tilde{u}_i \frac{\partial^2 \tilde{u}_j}{\partial x_d^2}}\,. \tag{29}$$

This relation will be used later in the modeling of the unknown terms that arise from the filtering process.

### IV.B. Approximation of Sub-analytical filter stress, $\widetilde{u'u'}$

Two types of approximations of $\widetilde{u'u'}$ will be examined; the Boussinesq approximation (a modification of which is the commonly used Smagorinsky model[9]) and the formula in the present study arising from purely mathematical derivations. An additional intention of the latter is to explore potential new directions for modeling the unknown terms.

Using Eq. (26) for $u_i'$, we compute $u_i'u_j'$ as

$$u_i'u_j' = \left( -\left(\frac{\Delta_t^2}{4\gamma}\right)\frac{\partial^2(\tilde{u}_i + u_i')}{\partial t^2} - \sum_{d=1}^{D}\left(\frac{\Delta_d^2}{4\gamma}\right)\frac{\partial^2(\tilde{u}_i + u_i')}{\partial x_d^2}\right) \times \left( -\left(\frac{\Delta_t^2}{4\gamma}\right)\frac{\partial^2(\tilde{u}_j + u_j')}{\partial t^2} - \sum_{d=1}^{D}\left(\frac{\Delta_d^2}{4\gamma}\right)\frac{\partial^2(\tilde{u}_j + u_j')}{\partial x_d^2}\right). \tag{30}$$

As assumed for Eq. (29), we neglect the high order derivatives for the fluctuations, and arrive at

$$\widetilde{u_i'u_j'} = \frac{\Delta_\tau^4}{16\gamma^2}\frac{\partial^2\widetilde{\tilde{u}_i}}{\partial t^2}\frac{\partial^2\widetilde{\tilde{u}_j}}{\partial t^2} + \frac{\Delta_t^2}{4\gamma}\sum_{d=1}^{D}\frac{\Delta_d^2}{4\gamma}\frac{\partial^2\widetilde{\tilde{u}_i}}{\partial x_d^2}\frac{\partial^2\widetilde{\tilde{u}_j}}{\partial t^2} + \frac{\Delta_\tau^2}{4\gamma}\frac{\partial^2\tilde{u}_i}{\partial t^2}\widetilde{\sum_{d=1}^{D}\frac{\Delta_d^2}{4\gamma}\frac{\partial^2\tilde{u}_j}{\partial x_d^2}} + \sum_{d=1}^{D}\frac{\Delta_d^2}{4\gamma}\frac{\partial^2\widetilde{\tilde{u}_i}}{\partial x_d^2}\widetilde{\sum_{d=1}^{D}\frac{\Delta_d^2}{4\gamma}\frac{\partial^2\tilde{u}_j}{\partial x_d^2}}. \tag{31}$$

Clearly, the terms, such as $\frac{\partial^2\tilde{u}_i'}{\partial t^2}\frac{\partial^2\tilde{u}_j}{\partial t^2}$ along with $\frac{\partial^2\tilde{u}_i'}{\partial t^2}\frac{\partial^2\tilde{u}_j'}{\partial t^2}$ are neglected for now as a starting point. However, more accurate mathematical handling of what should be the remaining terms and how these remaining terms are to be approximated will be investigated and reported in a follow-up study.

## V. Numerical Experimentation of Spatial-Temporal Filtering

For clarity, this investigation is focused on the viscous Burgers' equation.

### V.A. Numerical Analysis of the Relative Weights of Filtered Terms

The assumptions used for deriving Eq. (29) and Eq. (31) are that terms containing $u'$ contribute a negligible value to the computations. A similar assumption was made regarding the higher-order derivatives in Eq. (23). In order to properly utilize Eq. (29), Eq. (31), and Eq. (23), the validity of the assumptions used to derive these equations must be analyzed.

Conditions for the convergence of a Taylor series expansion of the filter terms such as the ones performed in Eq. (14) and Eq. (67) have been focused on for expansions of spatial filters and can be found in Sagaut.[10] It is expected that the necessary conditions for convergence of an expansion of a spatial-temporal filter would follow a similar form as those required for convergence of a spatial-filter expansion. Within the length constraint of this paper, a full analytical and numerical investigation is not possible. However, a follow-up investigation is focused on determining the characteristics of the higher-order filter terms using analytical functions and DNS data provided by Wu et al.[11,12]

### V.B. Spatial-Temporal Filtering Applied to Burgers' Equation

Burgers' equation provides a numerical test case for applying spatial-temporal filtering to a nonlinear partial differential equation and, specifically, for analyzing the stability of the resulting equation. The current study focuses on the one-dimensional form

$$\frac{\partial u}{\partial t} + \frac{1}{2}\frac{\partial uu}{\partial x} - \nu\frac{\partial^2 u}{\partial x^2} = g(x,t)\ , \tag{32}$$

where $u$ is the instantaneous velocity, $\nu$ is the kinematic viscosity of the fluid, and $g(x,t)$ is a forcing term. After applying spatial filtering, the Burgers' equation becomes

$$\frac{\partial \overline{u}}{\partial t} + \frac{1}{2}\frac{\partial \overline{uu}}{\partial x} - \nu\frac{\partial^2 \overline{u}}{\partial x^2} = \bar{g}(x,t)\ . \tag{33}$$

Utilizing Eq. (23), the nonlinear term (approximated up to second-order derivatives) is given by

$$\overline{uu} = \bar{u}\bar{u} + \frac{\Delta_x^2}{2\gamma}\left(\frac{\partial u}{\partial x}\right)\left(\frac{\partial u}{\partial x}\right)\ . \tag{34}$$

The resulting Burgers' equation (with $u = \overline{u} + u'$ substituted into the nonlinear term) is given as

$$\frac{\partial \bar{u}}{\partial t} + \frac{1}{2}\frac{\partial \bar{u}\bar{u}}{\partial x} - \nu\frac{\partial^2 \bar{u}}{\partial x^2} = \bar{g}(x,t) - \frac{\Delta_x^2}{4\gamma}\frac{\partial}{\partial x}\left(\left(\frac{\partial \overline{u}}{\partial x}\right)\left(\frac{\partial \overline{u}}{\partial x}\right)\right) - f(u') \ , \tag{35}$$

where $f(u')$ encompasses those terms containing the unresolvable component, $u'$, and is given by

$$f(u') = \frac{\Delta_x^2}{2\gamma}\left(\frac{\partial \overline{u}}{\partial x}\right)\left(\frac{\partial^2 u'}{\partial x^2}\right) + \frac{\Delta_x^2}{2\gamma}\left(\frac{\partial u'}{\partial x}\right)\left(\frac{\partial^2 \overline{u}}{\partial x^2}\right) + \frac{\Delta_x^2}{2\gamma}\left(\frac{\partial u'}{\partial x}\right)\left(\frac{\partial^2 u'}{\partial x^2}\right) \ . \tag{36}$$

After applying the FAST filtering, the Burgers' equation is identical to Eq. (33) except for the addition of temporal derivatives in the nonlinear term. The nonlinear term (approximated up to second-order derivatives) using Eq. (23) and a form of Eq. (29) and Eq. (31) is now given by

$$\overline{uu} = \bar{u}\bar{u} + \frac{\Delta_\tau^2}{2\gamma}\left(\frac{\partial u}{\partial t}\right)\left(\frac{\partial u}{\partial t}\right) + \frac{\Delta_x^2}{2\gamma}\left(\frac{\partial u}{\partial x}\right)\left(\frac{\partial u}{\partial x}\right) \ . \tag{37}$$

The resulting Burgers' equation (with $u = \overline{u} + u'$ substituted into the nonlinear term) is given as

$$\frac{\partial \bar{u}}{\partial t} + \frac{1}{2}\frac{\partial \bar{u}\bar{u}}{\partial x} - \nu\frac{\partial^2 \bar{u}}{\partial x^2} = \bar{g}(x,t) - \frac{\Delta_\tau^2}{4\gamma}\frac{\partial}{\partial x}\left(\left(\frac{\partial \overline{u}}{\partial t}\right)\left(\frac{\partial \overline{u}}{\partial t}\right)\right) - \frac{\Delta_x^2}{4\gamma}\frac{\partial}{\partial x}\left(\left(\frac{\partial \overline{u}}{\partial x}\right)\left(\frac{\partial \overline{u}}{\partial x}\right)\right) - f(u') \ , \tag{38}$$

where $f(u')$ encompasses those terms containing the unresolvable component, $u'$, and is given by

$$\begin{aligned} f(u') = & \frac{\Delta_\tau^2}{2\gamma}\left(\frac{\partial \overline{u}}{\partial t}\right)\left(\frac{\partial^2 u'}{\partial x \partial t}\right) + \frac{\Delta_x^2}{2\gamma}\left(\frac{\partial \overline{u}}{\partial x}\right)\left(\frac{\partial^2 u'}{\partial x^2}\right) \\ & + \frac{\Delta_\tau^2}{2\gamma}\left(\frac{\partial u'}{\partial t}\right)\left(\frac{\partial^2 \overline{u}}{\partial x \partial t}\right) + \frac{\Delta_x^2}{2\gamma}\left(\frac{\partial u'}{\partial x}\right)\left(\frac{\partial^2 \overline{u}}{\partial x^2}\right) \\ & + \frac{\Delta_\tau^2}{2\gamma}\left(\frac{\partial u'}{\partial t}\right)\left(\frac{\partial^2 u'}{\partial x \partial t}\right) + \frac{\Delta_x^2}{2\gamma}\left(\frac{\partial u'}{\partial x}\right)\left(\frac{\partial^2 u'}{\partial x^2}\right) \ . \end{aligned} \tag{39}$$

In addition to the analytical terms arising from the filtering, this study includes a simple model for $f(u')$. The Boussinesq approximation

$$\langle \overline{u'u'} \rangle = -\frac{\partial}{\partial x}\left(K \langle \frac{\partial \overline{u}}{\partial x} \rangle\right) \tag{40}$$

along with a constant eddy viscosity, $K$, is utilized for the SFS model. Combining the Boussinesq approximation with the FAST filtered Burgers' equation, we obtain

$$\frac{\partial \bar{u}}{\partial t} + \frac{1}{2}\frac{\partial \bar{u}\bar{u}}{\partial x} - \nu\frac{\partial^2 \bar{u}}{\partial x^2} = \bar{g}(x,t) - \frac{\Delta_\tau^2}{4\gamma}\frac{\partial}{\partial x}\left(\left(\frac{\partial \overline{u}}{\partial t}\right)\left(\frac{\partial \overline{u}}{\partial t}\right)\right) - \frac{\Delta_x^2}{4\gamma}\frac{\partial}{\partial x}\left(\left(\frac{\partial \overline{u}}{\partial x}\right)\left(\frac{\partial \overline{u}}{\partial x}\right)\right) + \frac{\partial}{\partial x}\left(K \langle \frac{\partial \overline{u}}{\partial x} \rangle\right) \ . \tag{41}$$

### V.C. Numerical Discretization of Unfiltered Burgers' Equation

Within this study, the viscous Burgers' equation is discretized using a fourth-order finite-volume based spatial discretization[13,14] and a standard fourth-order Runge-Kutta temporal discretization method. Following a finite-volume based spatial discretization of a general, conservation equation, one obtains

$$\frac{\mathrm{d}}{\mathrm{d}t}\langle \mathbf{U} \rangle_{\boldsymbol{i}} = -\frac{1}{\Delta x^d}\sum_{d=1}^{D}\left(\left(\langle \vec{\mathbf{F}} \rangle_{\boldsymbol{i}+\frac{1}{2}\boldsymbol{e}^d} - \langle \vec{\mathbf{F}} \rangle_{\boldsymbol{i}-\frac{1}{2}\boldsymbol{e}^d}\right) - \left(\langle \vec{\mathbf{G}} \rangle_{\boldsymbol{i}+\frac{1}{2}\boldsymbol{e}^d} - \langle \vec{\mathbf{G}} \rangle_{\boldsymbol{i}-\frac{1}{2}\boldsymbol{e}^d}\right)\right) + \langle \mathbf{S} \rangle_{\boldsymbol{i}} \ , \tag{42}$$

where, $\mathbf{U}$ is the vector of conservative solution quantities, $\vec{\mathbf{F}}$ is the vector of inviscid fluxes across each face in the discretization, $\vec{\mathbf{G}}$ is the vector of viscous fluxes across each face, $\mathbf{S}$ is a problem-dependent source term, $\langle \cdot \rangle_{\boldsymbol{i}}$ denotes a vector of cell-averaged values, $\langle \cdot \rangle_{\boldsymbol{i}+\frac{1}{2}\boldsymbol{e}^d}$ denotes a vector of face-averaged values, and $\Delta x$ is the spatial discretization size (not to be confused with the spatial filter width $\Delta_x$). For the one-dimensional, unfiltered Burgers' equation considered here, the resulting semi-discrete form will be

$$\frac{\mathrm{d}}{\mathrm{d}t}\langle u \rangle_i = -\frac{1}{\Delta x}\left(\frac{1}{2}\left(\langle uu \rangle_{i+\frac{1}{2}} - \langle uu \rangle_{i-\frac{1}{2}}\right) - \nu\left(\langle \frac{\partial u}{\partial x} \rangle_{i+\frac{1}{2}} - \langle \frac{\partial u}{\partial x} \rangle_{i-\frac{1}{2}}\right)\right) + \langle g(x,t) \rangle_i \ . \tag{43}$$

For a multi-dimensional case, the fourth-order inviscid fluxes are calculated using the product rule[13]

$$\langle uu\rangle_{i+\frac{1}{2}} = \langle u\rangle_{\boldsymbol{i}+\frac{1}{2}\boldsymbol{e}^d}\langle u\rangle_{\boldsymbol{i}+\frac{1}{2}\boldsymbol{e}^d} + \frac{h^2}{12}\sum_{d'\neq d}\frac{\partial u}{\partial x_{d'}}\frac{\partial v}{\partial x_{d'}} \ . \tag{44}$$

For the one-dimensional case, Eq. (44) reduces to

$$\langle uu\rangle_{i+\frac{1}{2}} = \langle u\rangle_{i+\frac{1}{2}}\langle u\rangle_{i+\frac{1}{2}} \ , \tag{45}$$

where the fourth-order face-averaged conservative quantities are calculated using

$$\langle u\rangle_{i+\frac{1}{2}} = \frac{7}{12}\left(\langle u\rangle_i + \langle u\rangle_{i+1}\right) - \frac{1}{12}\left(\langle u\rangle_{i-1} + \langle u\rangle_{i+2}\right) \ . \tag{46}$$

Finally, the fourth-order viscous fluxes in the one-dimensional case are calculated by

$$\langle\frac{\partial u}{\partial x}\rangle_{i+\frac{1}{2}} = \frac{1}{12\Delta x}\left(15\langle u\rangle_{i+1} - 15\langle u\rangle_i - \langle u\rangle_{i+2} + \langle u\rangle_{i-1}\right) \ . \tag{47}$$

### V.D. Numerical Discretization of Filtered Burgers' Equation

Filtering the Burgers' equation generates terms which must be modeled and consequently which must be discretized. In Eq. (38), spatial filtering generates one new analytical term which must be discretized (any empirically modeled terms arising from the filtering will be addressed later). This new term appears as

$$\text{Spatial Filtered Flux } = \frac{\Delta_x^2}{4\gamma}\frac{\partial}{\partial x}\left(\left(\frac{\partial\overline{u}}{\partial x}\right)\left(\frac{\partial\overline{u}}{\partial x}\right)\right) \ . \tag{48}$$

When viewed as a filter-flux, this term can be expanded using Eq. (45) and discretized as

$$\frac{\Delta_x^2}{4\gamma\Delta x}\left(\langle\frac{\partial\overline{u}}{\partial x}\frac{\partial\overline{u}}{\partial x}\rangle_{i+\frac{1}{2}} - \langle\frac{\partial\overline{u}}{\partial x}\frac{\partial\overline{u}}{\partial x}\rangle_{i-\frac{1}{2}}\right) = \frac{\Delta_x^2}{4\gamma\Delta x}\left(\langle\frac{\partial\overline{u}}{\partial x}\rangle_{i+\frac{1}{2}}\langle\frac{\partial\overline{u}}{\partial x}\rangle_{i+\frac{1}{2}} - \langle\frac{\partial\overline{u}}{\partial x}\rangle_{i-\frac{1}{2}}\langle\frac{\partial\overline{u}}{\partial x}\rangle_{i-\frac{1}{2}}\right) \ , \tag{49}$$

where the derivatives are computed by Eq. (47). The temporal filtering also generates one term

$$\text{Temporal Filtered Flux } = \frac{\Delta_\tau^2}{4\gamma}\frac{\partial}{\partial x}\left(\left(\frac{\partial\overline{u}}{\partial t}\right)\left(\frac{\partial\overline{u}}{\partial t}\right)\right) \ . \tag{50}$$

When viewed as another filter-flux, this term can be discretized similarly as

$$\frac{\Delta_\tau^2}{4\gamma\Delta x}\left(\langle\frac{\partial\overline{u}}{\partial t}\frac{\partial\overline{u}}{\partial t}\rangle_{i+\frac{1}{2}} - \langle\frac{\partial\overline{u}}{\partial t}\frac{\partial\overline{u}}{\partial t}\rangle_{i-\frac{1}{2}}\right) = \frac{\Delta_\tau^2}{4\gamma\Delta x}\left(\langle\frac{\partial\overline{u}}{\partial t}\rangle_{i+\frac{1}{2}}\langle\frac{\partial\overline{u}}{\partial t}\rangle_{i+\frac{1}{2}} - \langle\frac{\partial\overline{u}}{\partial t}\rangle_{i-\frac{1}{2}}\langle\frac{\partial\overline{u}}{\partial t}\rangle_{i-\frac{1}{2}}\right) \ , \tag{51}$$

where $\frac{\partial\overline{u}}{\partial t}$ can be further discretized using the centered scheme as done for the spatial derivative as

$$\langle\frac{\partial\overline{u}}{\partial t}\rangle_{i+\frac{1}{2}} = \frac{7}{12}\left(\langle\frac{\partial\overline{u}}{\partial t}\rangle_i + \langle\frac{\partial\overline{u}}{\partial t}\rangle_{i+1}\right) - \frac{1}{12}\left(\langle\frac{\partial\overline{u}}{\partial t}\rangle_{i-1} + \langle\frac{\partial\overline{u}}{\partial t}\rangle_{i+2}\right) \ . \tag{52}$$

In the one-dimensional case, the face-averages in Eq. (52) are equivalent to

$$\langle\frac{\partial\overline{u}}{\partial t}\rangle_{i+\frac{1}{2}} = \frac{7}{12}\left(\frac{\partial\langle\overline{u}\rangle_i}{\partial t} + \frac{\partial\langle\overline{u}\rangle_{i+1}}{\partial t}\right) - \frac{1}{12}\left(\frac{\partial\langle\overline{u}\rangle_{i-1}}{\partial t} + \frac{\partial\langle\overline{u}\rangle_{i+2}}{\partial t}\right) \ . \tag{53}$$

As a result, the left hand side (LHS) of the semi-discrete formulation of the Burgers' equation as shown in Eq. (43) would appear, after moving the temporal derivatives from the right hand side (RHS) to the LHS, as

$$\begin{aligned}\frac{\mathrm{d}}{\mathrm{d}t}\langle\overline{u}\rangle_i + \frac{\Delta_\tau^2}{576\gamma\Delta x}\Bigg(&\frac{\mathrm{d}\langle\overline{u}\rangle_{i+2}}{\mathrm{d}t}\frac{\mathrm{d}\langle\overline{u}\rangle_{i+2}}{\mathrm{d}t} - 14\frac{\mathrm{d}\langle\overline{u}\rangle_{i+2}}{\mathrm{d}t}\frac{\mathrm{d}\langle\overline{u}\rangle_{i+1}}{\mathrm{d}t} - 14\frac{\mathrm{d}\langle\overline{u}\rangle_{i+2}}{\mathrm{d}t}\frac{\mathrm{d}\langle\overline{u}\rangle_{i}}{\mathrm{d}t}\\ &+2\frac{\mathrm{d}\langle\overline{u}\rangle_{i+2}}{\mathrm{d}t}\frac{\mathrm{d}\langle\overline{u}\rangle_{i-1}}{\mathrm{d}t} + 48\frac{\mathrm{d}\langle\overline{u}\rangle_{i+1}}{\mathrm{d}t}\frac{\mathrm{d}\langle\overline{u}\rangle_{i+1}}{\mathrm{d}t} + 112\frac{\mathrm{d}\langle\overline{u}\rangle_{i+1}}{\mathrm{d}t}\frac{\mathrm{d}\langle\overline{u}\rangle_{i}}{\mathrm{d}t}\\ &-2\frac{\mathrm{d}\langle\overline{u}\rangle_{i+1}}{\mathrm{d}t}\frac{\mathrm{d}\langle\overline{u}\rangle_{i-2}}{\mathrm{d}t} - 48\frac{\mathrm{d}\langle\overline{u}\rangle_{i-1}}{\mathrm{d}t}\frac{\mathrm{d}\langle\overline{u}\rangle_{i-1}}{\mathrm{d}t} - 112\frac{\mathrm{d}\langle\overline{u}\rangle_{i-1}}{\mathrm{d}t}\frac{\mathrm{d}\langle\overline{u}\rangle_{i}}{\mathrm{d}t}\\ &-\frac{\mathrm{d}\langle\overline{u}\rangle_{i-2}}{\mathrm{d}t}\frac{\mathrm{d}\langle\overline{u}\rangle_{i-2}}{\mathrm{d}t} + 14\frac{\mathrm{d}\langle\overline{u}\rangle_{i-2}}{\mathrm{d}t}\frac{\mathrm{d}\langle\overline{u}\rangle_{i-1}}{\mathrm{d}t} + 14\frac{\mathrm{d}\langle\overline{u}\rangle_{i-2}}{\mathrm{d}t}\frac{\mathrm{d}\langle\overline{u}\rangle_{i}}{\mathrm{d}t}\Bigg)\end{aligned} \tag{54}$$

where $\frac{\partial}{\partial t}$ has become $\frac{\mathrm{d}}{\mathrm{d}t}$ due to the change from a partial differential equation to an ordinary differential equation after spatial discretization.

### V.E. Jacobian Matrix for Numerical Stability Analysis of Burgers' Equation

In order to understand the effect of the spatial-temporal filtering on the stability of Burgers' equation, a stability analysis must be performed. Due to the nonlinear nature of Burgers' equation, the stability analysis performed herein will be in the discrete sense, that is, the stability information will be for a given solution state. The exact reasons for this will become evident shortly.

To approximate the stability of the nonlinear Burgers' equation, the solution is expanded about a point in space and time. Retaining the first-order derivatives and locally linearizing in time, the resulting expansion is

$$\frac{\mathrm{d}}{\mathrm{d}t}\langle u\rangle_i = \frac{\mathrm{d}}{\mathrm{d}t}\langle u\rangle_i^n + \nabla\left(\frac{\mathrm{d}}{\mathrm{d}t}\langle u\rangle_i^n\right)\left(\langle u\rangle_i - \langle u\rangle_i^n\right) \ , \tag{55}$$

where $n$ is the given time-step that the solution is expanded about. The eigenvalues of the Jacobian matrix in Eq. (55) are examined in order to gain insight into the stability of the equation. As previously defined, $\langle u\rangle_i$ is a vector of the cell-averaged conservative solution quantity. Therefore, for a discretization of cells ranging from 0 to $N$, the Jacobian matrix will take the form

$$\nabla\left(\frac{\mathrm{d}}{\mathrm{d}t}\langle u\rangle_i^n\right) = \begin{bmatrix} \frac{\partial}{\partial\langle u\rangle_0^n}\left(\frac{\mathrm{d}}{\mathrm{d}t}\langle u\rangle_0^n\right) & \frac{\partial}{\partial\langle u\rangle_1^n}\left(\frac{\mathrm{d}}{\mathrm{d}t}\langle u\rangle_0^n\right) & \cdots & \frac{\partial}{\partial\langle u\rangle_N^n}\left(\frac{\mathrm{d}}{\mathrm{d}t}\langle u\rangle_0^n\right) \\ \frac{\partial}{\partial\langle u\rangle_0^n}\left(\frac{\mathrm{d}}{\mathrm{d}t}\langle u\rangle_1^n\right) & \frac{\partial}{\partial\langle u\rangle_1^n}\left(\frac{\mathrm{d}}{\mathrm{d}t}\langle u\rangle_1^n\right) & \cdots & \frac{\partial}{\partial\langle u\rangle_N^n}\left(\frac{\mathrm{d}}{\mathrm{d}t}\langle u\rangle_1^n\right) \\ \cdots & \cdots & \ddots & \vdots \\ \frac{\partial}{\partial\langle u\rangle_0^n}\left(\frac{\mathrm{d}}{\mathrm{d}t}\langle u\rangle_N^n\right) & \frac{\partial}{\partial\langle u\rangle_1^n}\left(\frac{\mathrm{d}}{\mathrm{d}t}\langle u\rangle_N^n\right) & \cdots & \frac{\partial}{\partial\langle u\rangle_N^n}\left(\frac{\mathrm{d}}{\mathrm{d}t}\langle u\rangle_N^n\right) \end{bmatrix} . \tag{56}$$

To construct this matrix, the semi-discrete form of the numerical discretization must be known and the derivatives need to be computed. For the fourth-order discretization used in this work, the derivatives of the semi-discrete form are given as

$$\frac{\partial}{\partial\langle u\rangle_{i-2}^n}\left(\frac{\mathrm{d}}{\mathrm{d}t}\langle u\rangle_i^n\right) = \frac{1}{144\Delta x}\left(\langle u\rangle_{i+1}^n - 7\langle u\rangle_i^n - 7\langle u\rangle_{i-1}^n + \langle u\rangle_{i-2}^n\right) - \frac{\nu}{12\Delta x^2} \tag{57a}$$

$$\frac{\partial}{\partial\langle u\rangle_{i-1}^n}\left(\frac{\mathrm{d}}{\mathrm{d}t}\langle u\rangle_i^n\right) = \frac{1}{144\Delta x}\left(-\langle u\rangle_{i+2}^n + 56\langle u\rangle_i^n + 48\langle u\rangle_{i-1}^n - 7\langle u\rangle_{i-2}^n\right) + \frac{4\nu}{3\Delta x^2} \tag{57b}$$

$$\frac{\partial}{\partial\langle u\rangle_i^n}\left(\frac{\mathrm{d}}{\mathrm{d}t}\langle u\rangle_i^n\right) = \frac{1}{144\Delta x}\left(7\langle u\rangle_{i+2}^n - 56\langle u\rangle_{i+1}^n + 56\langle u\rangle_{i-1}^n - 7\langle u\rangle_{i-2}^n\right) - \frac{5\nu}{2\Delta x^2} \tag{57c}$$

$$\frac{\partial}{\partial\langle u\rangle_{i+1}^n}\left(\frac{\mathrm{d}}{\mathrm{d}t}\langle u\rangle_i^n\right) = \frac{1}{144\Delta x}\left(7\langle u\rangle_{i+2}^n - 48\langle u\rangle_{i+1}^n - 56\langle u\rangle_i^n + \langle u\rangle_{i-2}^n\right) + \frac{4\nu}{3\Delta x^2} \tag{57d}$$

$$\frac{\partial}{\partial\langle u\rangle_{i+2}^n}\left(\frac{\mathrm{d}}{\mathrm{d}t}\langle u\rangle_i^n\right) = \frac{1}{144\Delta x}\left(-\langle u\rangle_{i+2}^n + 7\langle u\rangle_{i+1}^n + 7\langle u\rangle_i^n - \langle u\rangle_{i-1}^n\right) - \frac{\nu}{12\Delta x^2} \tag{57e}$$

where all the derivatives of $\frac{\mathrm{d}}{\mathrm{d}t}\langle u\rangle_i^n$ with respect to other points are zero. Each term from Eq. (57) can be substituted into Eq. (56) in order to calculate the eigenvalues of the Jacobian matrix. The eigenvalues can be computed for any solution states. Although this process does not show stability in every case, it still provides general, qualitative stability behavior for numerical tests that are of interest.

### V.F. Jacobian Matrix for Numerical Stability Analysis of the Spatially-Filtered Burgers' Equation

The spatially-filtered Burgers' equation includes extra terms that arise due to the spatial filtering. These terms must be dealt with in the discretization and the stability analysis. Including these terms in the derivatives provides new equations that are slightly different from Eq. (57). The additional terms that are generated in the derivatives can be added to the terms shown in Eq. (57) (where the terms in Eq. (57) will

all switch from $u$ to $\overline{u}$) as

$$
\begin{aligned}
\frac{\partial}{\partial\langle\overline{u}\rangle_{i-2}^{n}}\left(\frac{\mathrm{d}}{\mathrm{d}t}\langle\overline{u}\rangle_{i}^{n}\right) &= \text{Eq. (57a)} + \frac{\Delta_x^2}{288\gamma\Delta x^3}\left(-\langle\overline{u}\rangle_{i+1}^{n} + 15\langle\overline{u}\rangle_{i}^{n} - 15\langle\overline{u}\rangle_{i-1}^{n} + \langle\overline{u}\rangle_{i-2}^{n}\right)\\
\frac{\partial}{\partial\langle\overline{u}\rangle_{i-1}^{n}}\left(\frac{\mathrm{d}}{\mathrm{d}t}\langle\overline{u}\rangle_{i}^{n}\right) &= \text{Eq. (57b)} + \frac{\Delta_x^2}{288\gamma\Delta x^3}\left(\langle\overline{u}\rangle_{i+2}^{n} - 210\langle\overline{u}\rangle_{i}^{n} + 224\langle\overline{u}\rangle_{i-1}^{n} - 15\langle\overline{u}\rangle_{i-2}^{n}\right)\\
\frac{\partial}{\partial\langle\overline{u}\rangle_{i}^{n}}\left(\frac{\mathrm{d}}{\mathrm{d}t}\langle\overline{u}\rangle_{i}^{n}\right) &= \text{Eq. (57c)} + \frac{\Delta_x^2}{288\gamma\Delta x^3}\left(-15\langle\overline{u}\rangle_{i+2}^{n} + 210\langle\overline{u}\rangle_{i+1}^{n} - 210\langle\overline{u}\rangle_{i-1}^{n} + 15\langle\overline{u}\rangle_{i-2}^{n}\right)\\
\frac{\partial}{\partial\langle\overline{u}\rangle_{i+1}^{n}}\left(\frac{\mathrm{d}}{\mathrm{d}t}\langle\overline{u}\rangle_{i}^{n}\right) &= \text{Eq. (57d)} + \frac{\Delta_x^2}{288\gamma\Delta x^3}\left(15\langle\overline{u}\rangle_{i+2}^{n} - 224\langle\overline{u}\rangle_{i+1}^{n} + 210\langle\overline{u}\rangle_{i}^{n} - \langle\overline{u}\rangle_{i-2}^{n}\right)\\
\frac{\partial}{\partial\langle\overline{u}\rangle_{i+2}^{n}}\left(\frac{\mathrm{d}}{\mathrm{d}t}\langle\overline{u}\rangle_{i}^{n}\right) &= \text{Eq. (57e)} + \frac{\Delta_x^2}{288\gamma\Delta x^3}\left(-\langle\overline{u}\rangle_{i+2}^{n} + 15\langle\overline{u}\rangle_{i+1}^{n} - 15\langle\overline{u}\rangle_{i}^{n} + \langle\overline{u}\rangle_{i-1}^{n}\right)
\end{aligned}
\tag{58}
$$

### V.G. Jacobian Matrix for Numerical Stability Analysis of the Spatially-Temporally-Filtered Burgers' Equation

As seen in Eq. (54), the spatial-temporal filtering generates temporal derivatives that modify the form of the LHS of the filtered, semi-discrete governing equation. In order to incorporate this change into the stability analysis, the LHS of the system will be written in matrix form given by

$$
B_p(a,b,c,d,e)\left(\overrightarrow{\frac{\mathrm{d}}{\mathrm{d}t}\langle\overline{u}\rangle}\right) \tag{59}
$$

where $B_p(\cdot)$ denotes a banded matrix for a periodic domain, $\overrightarrow{\frac{\mathrm{d}}{\mathrm{d}t}\langle\overline{u}\rangle}$ is a vector of the temporal derivatives at each point, and $a, b, c, d$, and $e$ are the diagonals ($c$ being the main diagonal). Due to the nonlinearity in this matrix, elements $a, b, c, d$, and $e$ can be formulated in many different ways. The formulation of these terms utilized within the present study is given as

$$
\begin{aligned}
a &= \frac{\Delta_\tau^2}{576\gamma\Delta x}\left(-\frac{\mathrm{d}\langle\overline{u}\rangle_{i-2}}{\mathrm{d}t}\right)\\
b &= \frac{\Delta_\tau^2}{576\gamma\Delta x}\left(-48\frac{\mathrm{d}\langle\overline{u}\rangle_{i-1}}{\mathrm{d}t} + 14\frac{\mathrm{d}\langle\overline{u}\rangle_{i-2}}{\mathrm{d}t} - 14\frac{\mathrm{d}\langle\overline{u}\rangle_{i}}{\mathrm{d}t} + 2\frac{\mathrm{d}\langle\overline{u}\rangle_{i+2}}{\mathrm{d}t}\right)\\
c &= 1 + \frac{\Delta_\tau^2}{576\gamma\Delta x}\left(14\frac{\mathrm{d}\langle\overline{u}\rangle_{i-2}}{\mathrm{d}t} - 98\frac{\mathrm{d}\langle\overline{u}\rangle_{i-1}}{\mathrm{d}t} + 98\frac{\mathrm{d}\langle\overline{u}\rangle_{i+1}}{\mathrm{d}t} - 14\frac{\mathrm{d}\langle\overline{u}\rangle_{i+2}}{\mathrm{d}t}\right)\\
d &= \frac{\Delta_\tau^2}{576\gamma\Delta x}\left(48\frac{\mathrm{d}\langle\overline{u}\rangle_{i+1}}{\mathrm{d}t} - 2\frac{\mathrm{d}\langle\overline{u}\rangle_{i-2}}{\mathrm{d}t} + 14\frac{\mathrm{d}\langle\overline{u}\rangle_{i}}{\mathrm{d}t} - 14\frac{\mathrm{d}\langle\overline{u}\rangle_{i+2}}{\mathrm{d}t}\right)\\
e &= \frac{\Delta_\tau^2}{576\gamma\Delta x}\left(\frac{\mathrm{d}\langle\overline{u}\rangle_{i+2}}{\mathrm{d}t}\right) \ .
\end{aligned}
\tag{60}
$$

After formulating this matrix, the entire semi-discrete form can be written in the form

$$
B_p(a,b,c,d,e)\left(\overrightarrow{\frac{\mathrm{d}}{\mathrm{d}t}\langle\overline{u}\rangle_i}\right) = \text{RHS} \tag{61}
$$

where RHS is the vector. The diagonal matrix, $B_p$, is then inverted and multiplied to the RHS, resulting in

$$
\overrightarrow{\frac{\mathrm{d}}{\mathrm{d}t}\langle\overline{u}\rangle_i} = B_p^{-1}(a,b,c,d,e)\,(\text{RHS})\,. \tag{62}
$$

When performing the stability analysis, Eq. (55) is still utilized and the $B_p$ matrix is filled with values from the current time. In this way, the Jacobian matrix Eq. (56) provides a qualitative assessment of the stability for any given solution state.

### V.H. Results of Nonlinear Stability Analysis of Unfiltered and Filtered Burgers' Equation

Given a solution state and following the stability analysis outlined above, we are readily able to obtain a stability contour for any wave number, up to the Nyquist frequency, with certain fluid properties, flow properties, and numerical setups specified. The results of the nonlinear stability analysis presented herein are for a computational mesh size of 500 and an initial waveform consisting of a single sine wave with an amplitude of $\omega_{\mathrm{A}}$, a mean value given by $\bar{\omega}$, and a wavenumber $\kappa$. The specified waveform data is given by

$$\omega = \bar{\omega} + \omega_{\mathrm{A}} \sin(2\pi\kappa x) \tag{63}$$

In each of Figs. 2–6, the complex plane of $\lambda\Delta t$ is displayed for the filtering schemes, with the stability contour of the standard Runge-Kutta (RK4) method in the background as a reference since this study employs the RK4 time marching method. Note that $\lambda' s$ are the eigenvalues of the Jacobian matrices from Sections V.E - V.G. For convenience when interpreting Figs. 2–6, the legend used in each is specified in Table 1.

Table 1: The symbol table for Figs. 2–6.

| Symbol | Equation # | |
|---|---|---|
| ○ | Eq. (32) | Burgers' equation |
| ○ | Eq. (35) | Spatially-filtered Burgers' equation |
| ○ | Eq. (38) | FAST Burgers' equation |
| × | Eq. (41) | FAST Burgers' equation with a model by Boussinesq approximation |

Figure 2 shows the complex plane for a case where the convection dominates the flow physics, with a relatively low kinematic viscosity of $\nu = 1.0\times10^{-6}$ m$^2$/s, $\bar{\omega} = 10$, $\omega_{\mathrm{A}} = 1$, and CFL = 1.0. As expected, $\lambda' s$ from all schemes are lying along the imaginary axis. An arbitrary wave number $\kappa = 70$ is used as a reference to show that little difference in the contours is seen for all wave numbers. For a diffusion dominated case as shown in Fig. 3, the distribution of eigenvalues for all schemes remains nearly the same and along the negative real axis. This is consistent with the physics. For $\kappa \geq 100$, however, the distribution slightly extends further to the left of $\mathbb{R}(\Delta t\lambda)$ = -2. When the convection and diffusion are competing processes, the patterns for the $\lambda\Delta t$-complex planes begin to differ substantially for the filtering and modeling methods. A representative stability contour plane is illustrated by Fig. 4, where $\omega_{\mathrm{A}} = 1$, $\bar{\omega} = 0.5$, $\nu = 0.001$m$^2$/s, CFL = 1.25, and von Neumann number = 0.5. While keeping the same style in Figs. 5 - 6, the figures are focused more on the $\lambda\Delta t$ contours for better comparison.

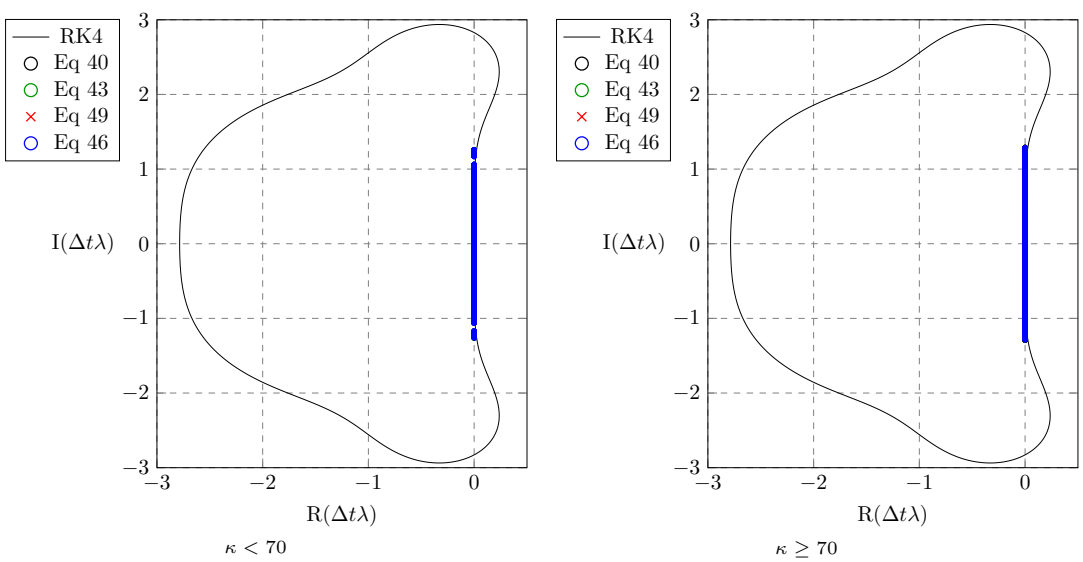


Figure 2: Convection dominated case: $\bar{\omega} = 10.0$, $\omega_{\mathrm{A}} = 1.0$, $\nu = 1.0\times10^{-6}$ m$^2$/s, CFL = 1.0

Both the $\omega_{\mathrm{A}}$ and the diffusion coefficient are larger in the case as shown in Fig. 5 than that in Fig. 6. The contours are shown for a range of wave numbers—purposely and arbitrarily selecting low and high,

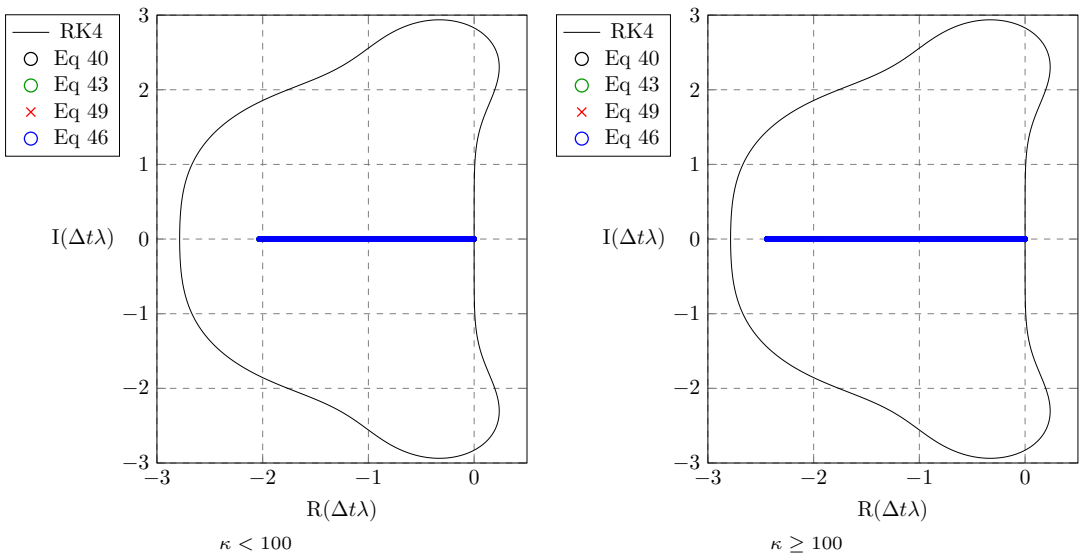


Figure 3: Diffusion dominated case: $\bar{\omega} = 1.0$, $\omega_{\mathrm{A}} = 1.0$, $\nu = 0.5\mathrm{m}^2/\mathrm{s}$, von Neumann number = 0.4

odd and even numbers. Apparent differences in the filtering methods are observed in both cases, while the FAST filtering method displays much larger variations within the distribution of the eigenvalues from the original (unfiltered) equation. In all cases, the stability of both filtering methods is comparable and the stability of the FAST filtering method is overall slightly improved. Figure 6 demonstrates a case, providing an interesting test on the capability of the filtering methods. For this particular case, the mean velocity of 0.5 and the sine wave amplitude of 1 guarantee that the flow field will have a periodic distribution of left moving and right moving flow, creating a shock-expansion-shock-expansion pattern. Whether or not this would occur in reality or is physically possible, it deliberately creates a challenging scenario for numerical stability. Nevertheless, it is clear from the stability analysis that our discretization and filtering methods still provide a decent stability region.

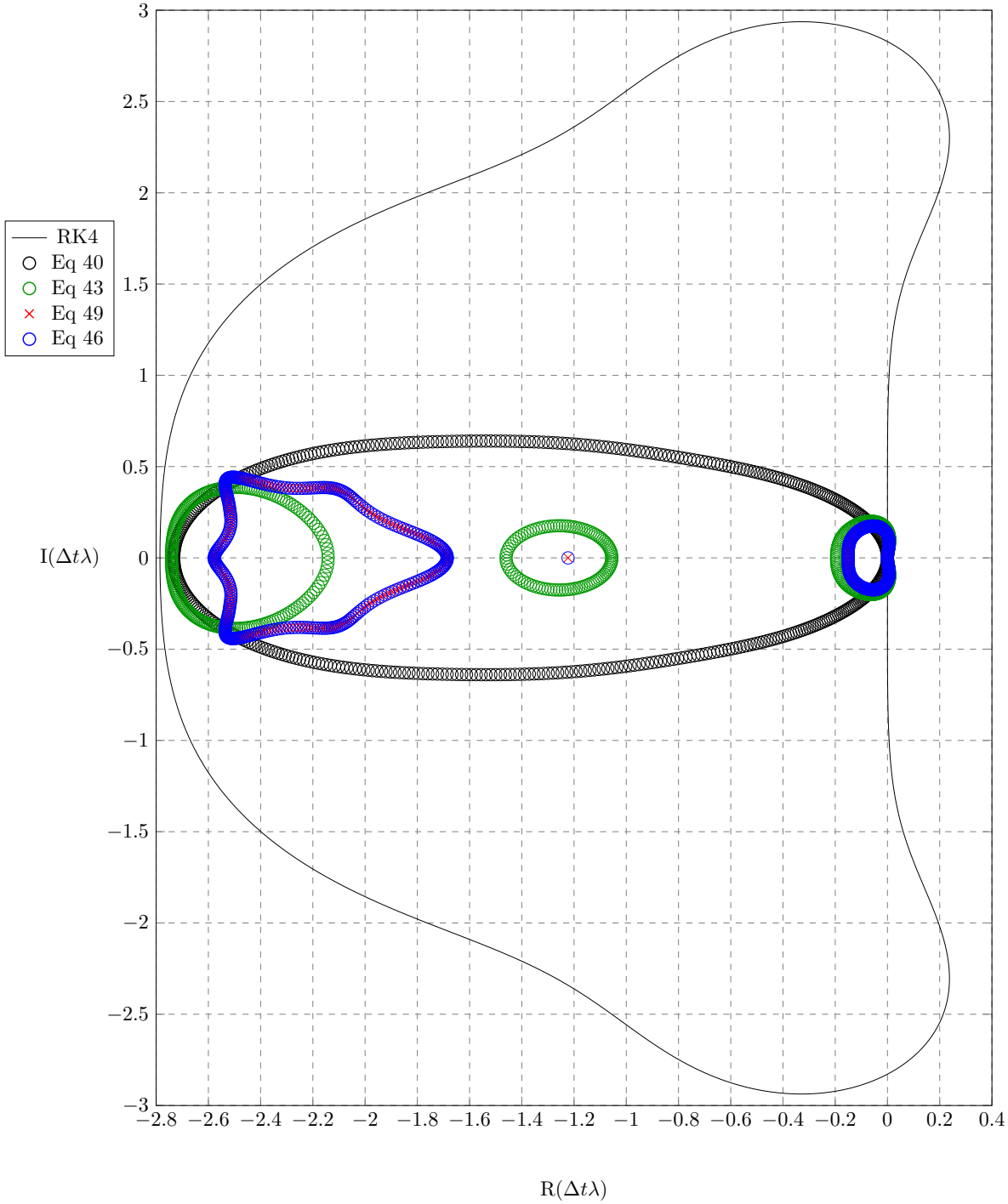


Figure 4: Convection-diffusion case: $\bar{\omega} = 0.5$, $\omega_{\mathrm{A}} = 1.0$, $\nu = 0.001\mathrm{m}^2/\mathrm{s}$, CFL = 1.25 and von Neumann number = 0.5

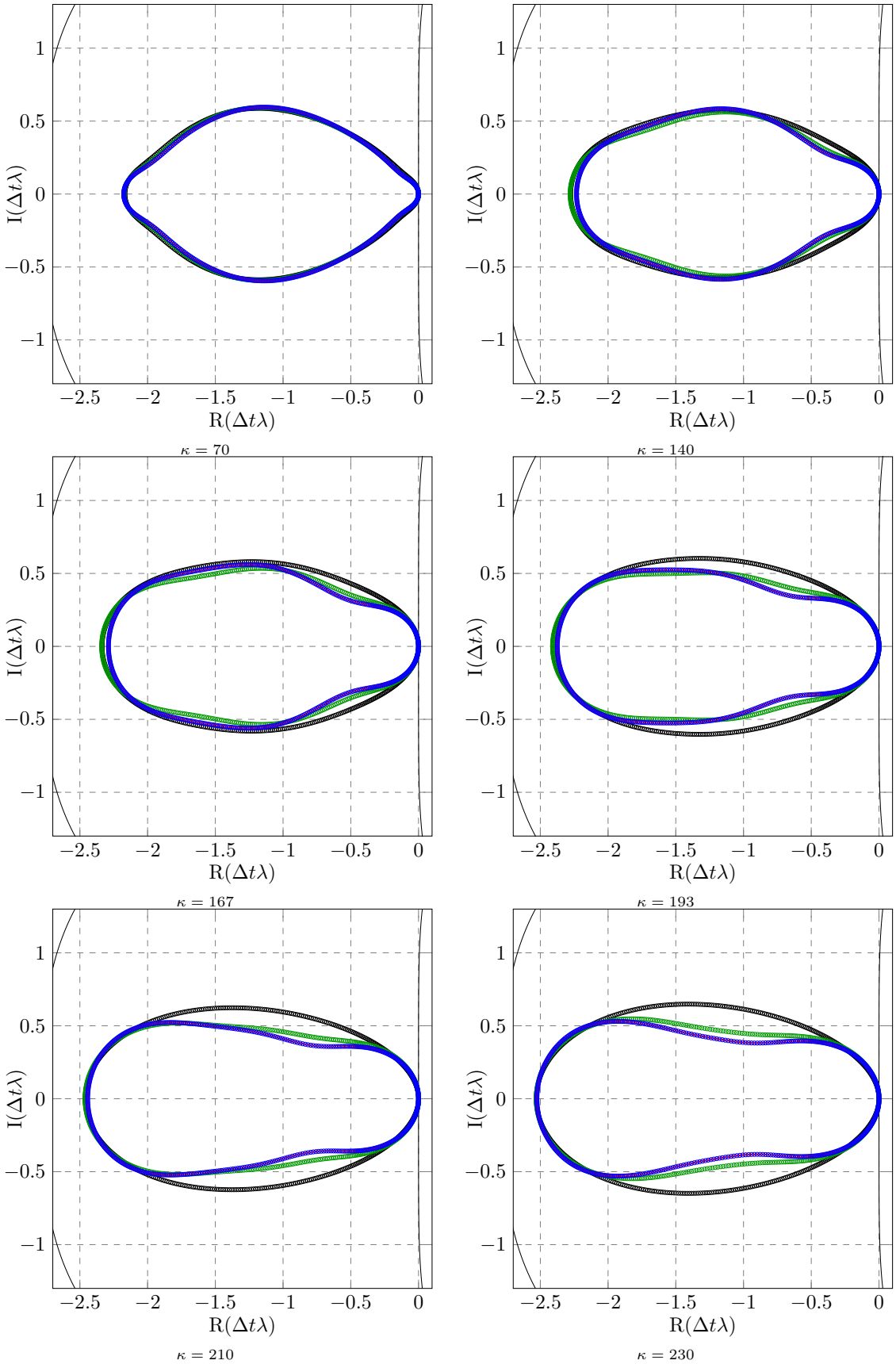


Figure 5: Convection-diffusion case: $\bar{\omega} = 1.0$, $\omega_{\mathrm{A}} = 1.0$, $\nu = 0.002\mathrm{m}^2/\mathrm{s}$, CFL $= 0.8$ and von Neumann number $= 0.45$

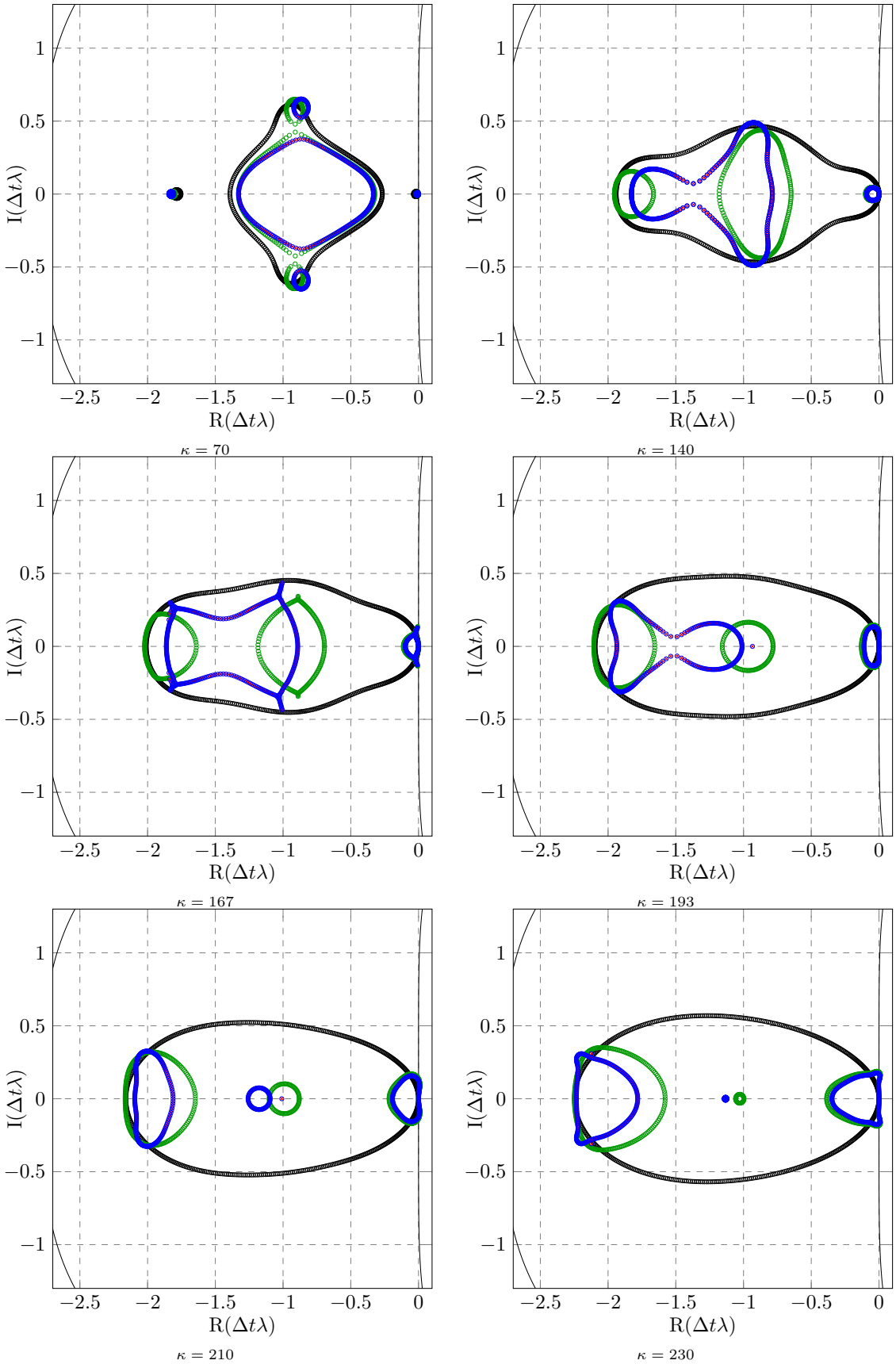


Figure 6: Convection-diffusion case: $\bar{\omega} = 0.5$, $\omega_{\mathrm{A}} = 1.0$, $\nu = 0.001\mathrm{m}^2/\mathrm{s}$, CFL = 1.0 and von Neumann number = 0.4

### V.I. Numerical Results of the Spatially-Temporally Filtered Burgers' Equation

Within this study, a spatially-temporally varying source term is specified for the viscous Burgers' equation. This forcing term provides an additional method by which the differences between the filtered and unfiltered equations become more apparent. The forcing term, $g(x,t)$, and the initial condition, $\omega_0$, are given by

$$\begin{aligned} g(x,t) &= 2 + \frac{19}{5}\sin(46\pi x + 74\pi t) + \frac{8}{5}\sin(140\pi x + 20\pi t + \frac{1}{4}) \\ &\quad + \frac{24}{5}\sin(120\pi x + 22\pi t)\sin(204\pi x + 60\pi t)\ , \end{aligned} \tag{64}$$

$$\begin{aligned} \omega_0 &= 30 + \frac{13}{5}\sin(54\pi x) + \frac{11}{5}\sin(100\pi x + 0.2) + \frac{23}{5}\sin(140\pi x + 0.05) + \frac{13}{4}\sin(240\pi x + 0.6) \\ &\quad + \frac{12}{5}\sin(380\pi x + 1.2) + \frac{41}{10}\sin(460\pi x + 0.3) + \frac{27}{10}\sin(540\pi x + 0.9) + \frac{39}{10}\sin(760\pi x + 0.5) \\ &\quad + \frac{6}{5}\sin(1020\pi x + 0.1) + \frac{4}{5}\sin(1380\pi x + 2) + \frac{7}{5}\sin(1660\pi x + 1.7)\ . \end{aligned} \tag{65}$$

For the simulations performed here, the kinematic viscosity is $1\times10^{-5}$, the eddy viscosity utilized in the

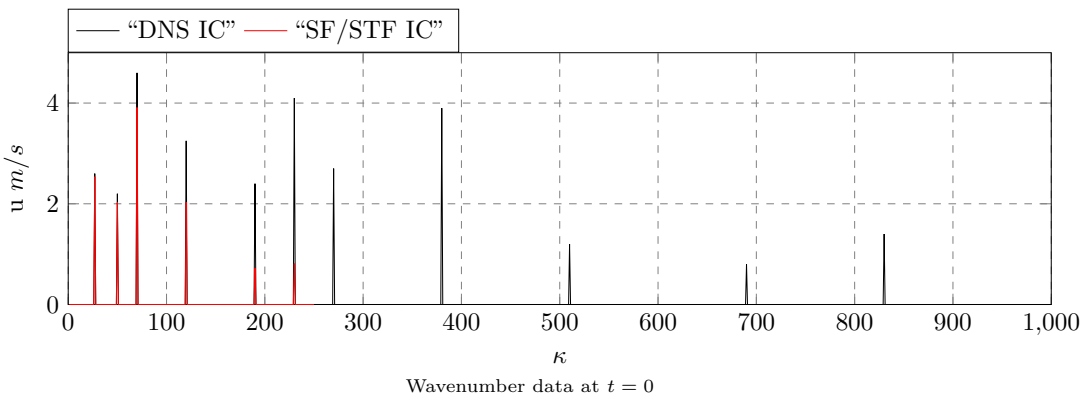


Figure 7: Initial condition: wavenumber spectrum

SFS model is $2\times10^{-7}$, and the temporal eddy viscosity utilized in the modified SFS model is $2\times10^{-7}$. The simulations are performed on two sets of grids, both with $0 \le x \le 1$. The first, used to resolve all flow scales, contains 100000 cells. The second, much coarser grid, contains 500 cells. Within the following figures, the solution on the fine grid is referred to as the "DNS" solution. The solution of the spatially-filtered Burgers' equation, Eq. (35), is referred to by "SF" (this utilizes the Boussinesq SFS approximation), while the solution of the spatially-temporally-filtered Burgers' equation, Eq. (38), is referred to by "STF" (this also utilizes the Boussinesq SFS approximation). Figure 7 presents the wavenumber decomposition of the initial condition on both the fine grid and the coarse grid. As for the filter sizes utilized here, two cases are presented. In one case, the spatial filter width, $\Delta_x$, is chosen to be twice the size of the spatial discretization size, $\Delta_x = 2\Delta x$, and the temporal filter width, $\Delta_\tau$, is chosen to be twice the temporal discretization width, $\Delta_\tau = 2\Delta t$. For the second case, the filter widths are chosen as $\Delta_x = 8\Delta x$ and $\Delta_\tau = 8\Delta t$. It is expected that the second case, providing a better separation of the unresolved scales from the resolved scales, will clearly demonstrate the variation between the spatially filtered and the spatially-temporally filtered equations.

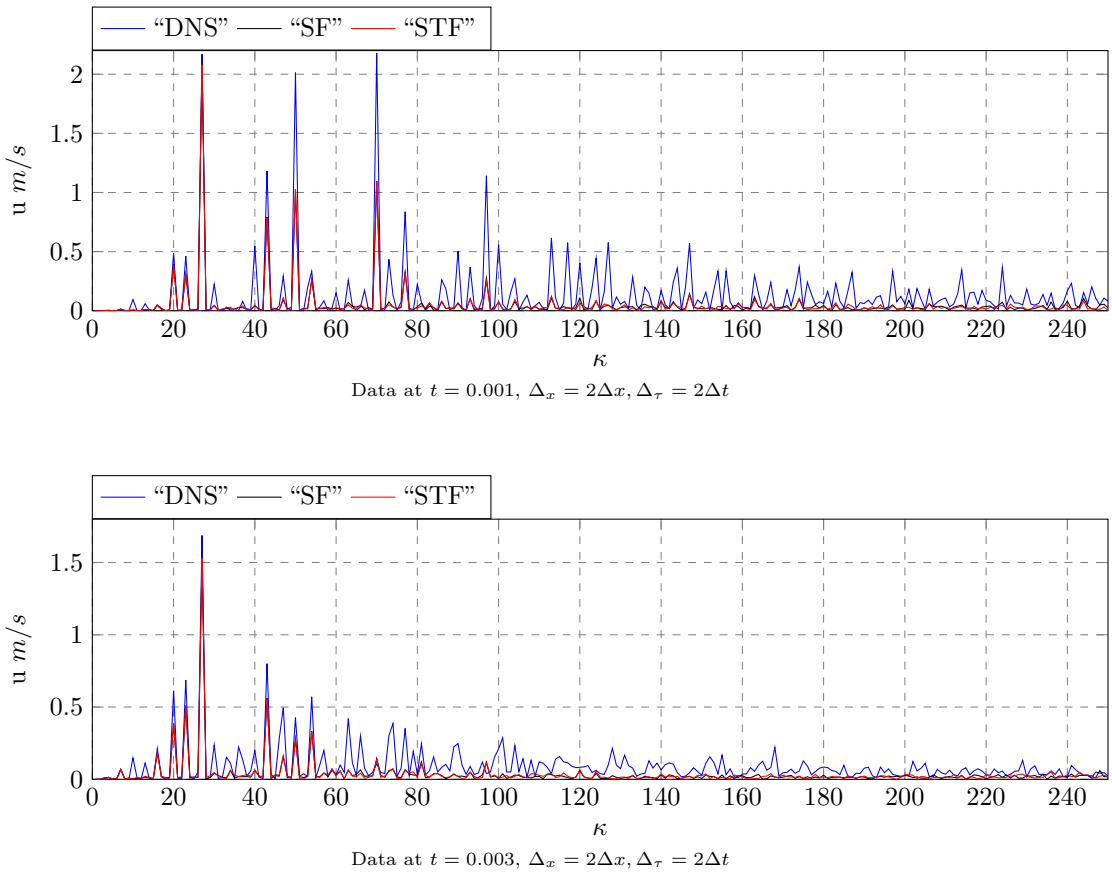


Figure 8: Comparison of wavenumbers from FFT of solutions

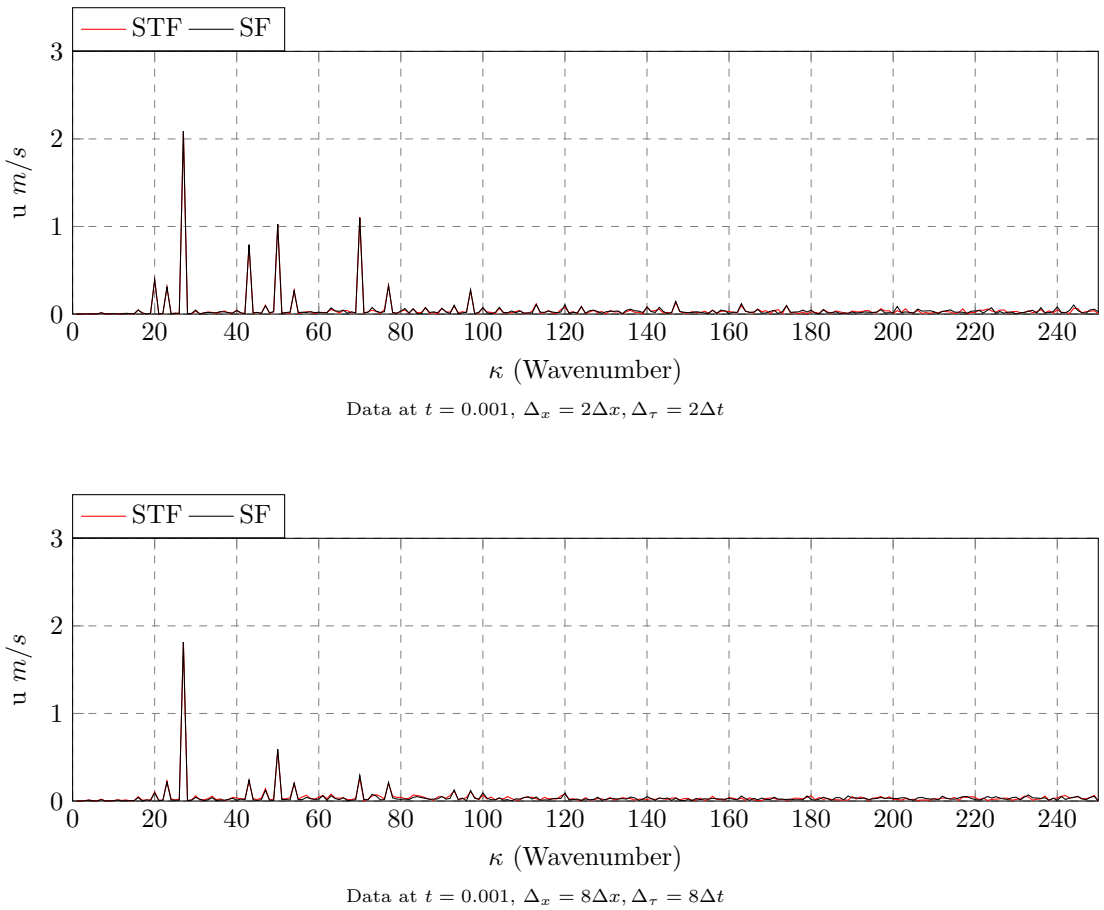


Figure 9: Comparison of wavenumbers from FFT of solutions using different filter sizes

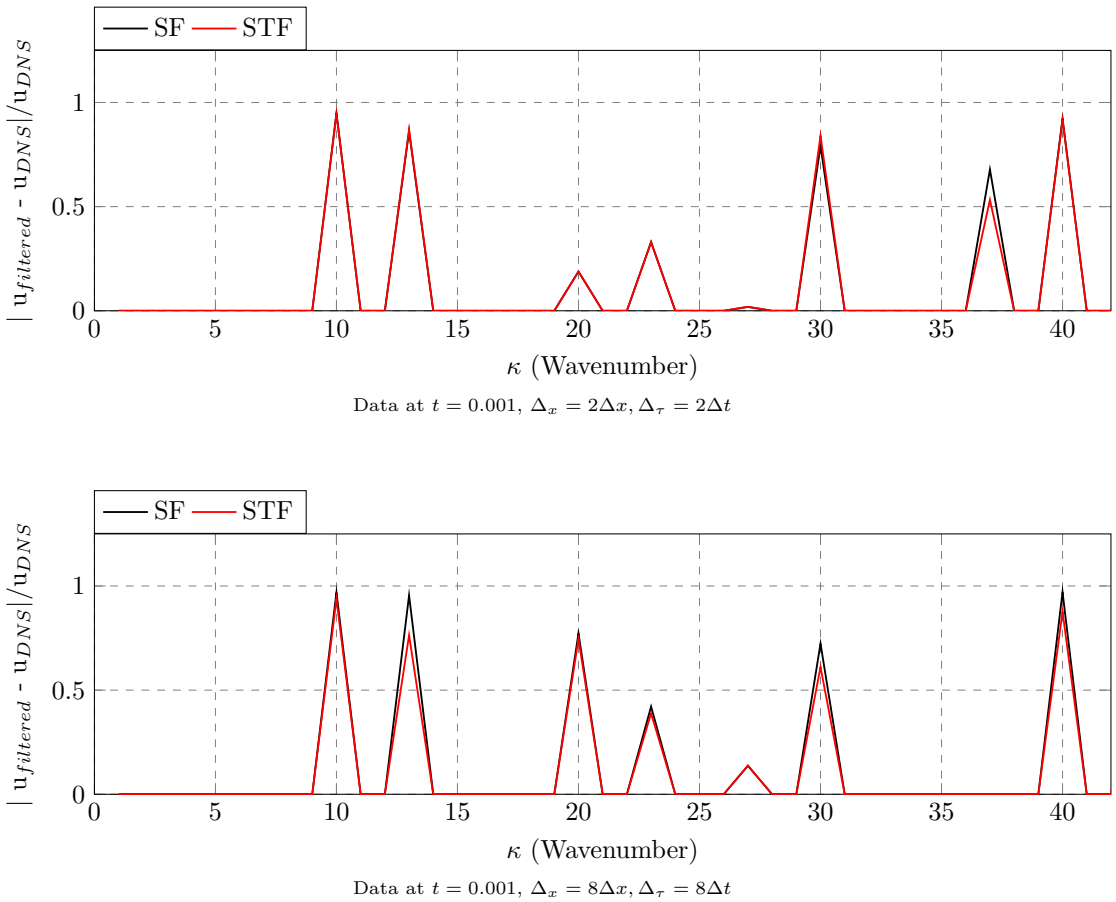


Figure 10: Normalized difference between "DNS" and filtered solutions using different filter sizes

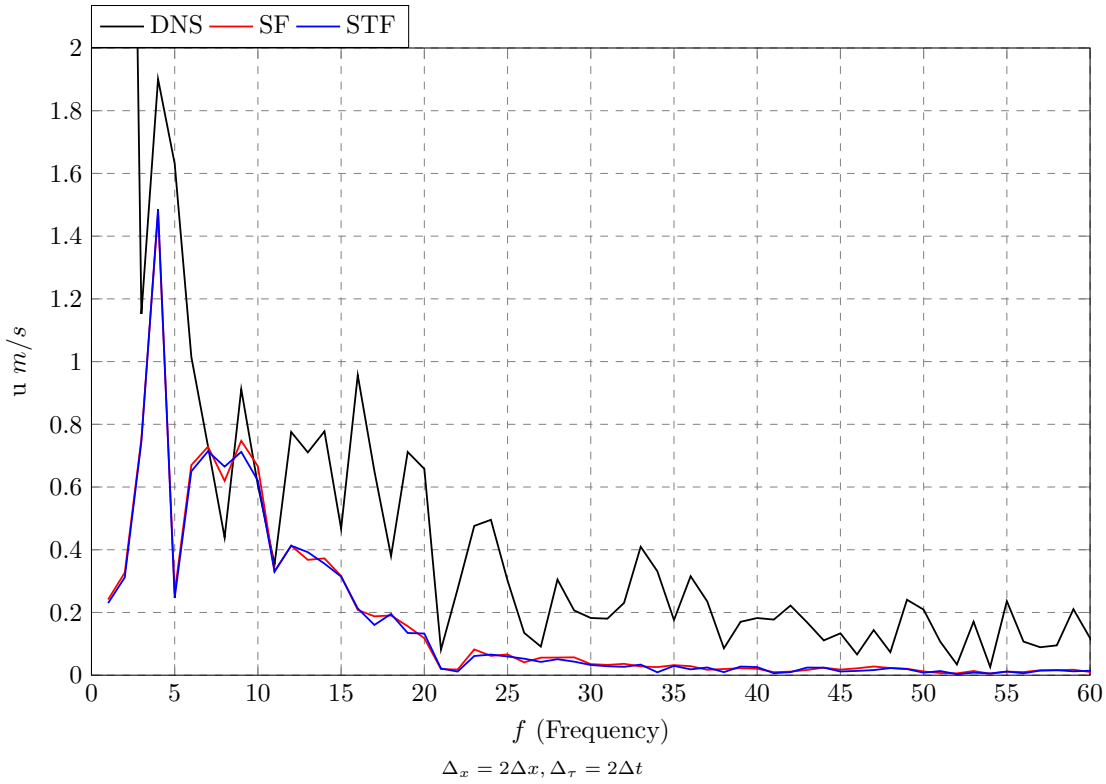


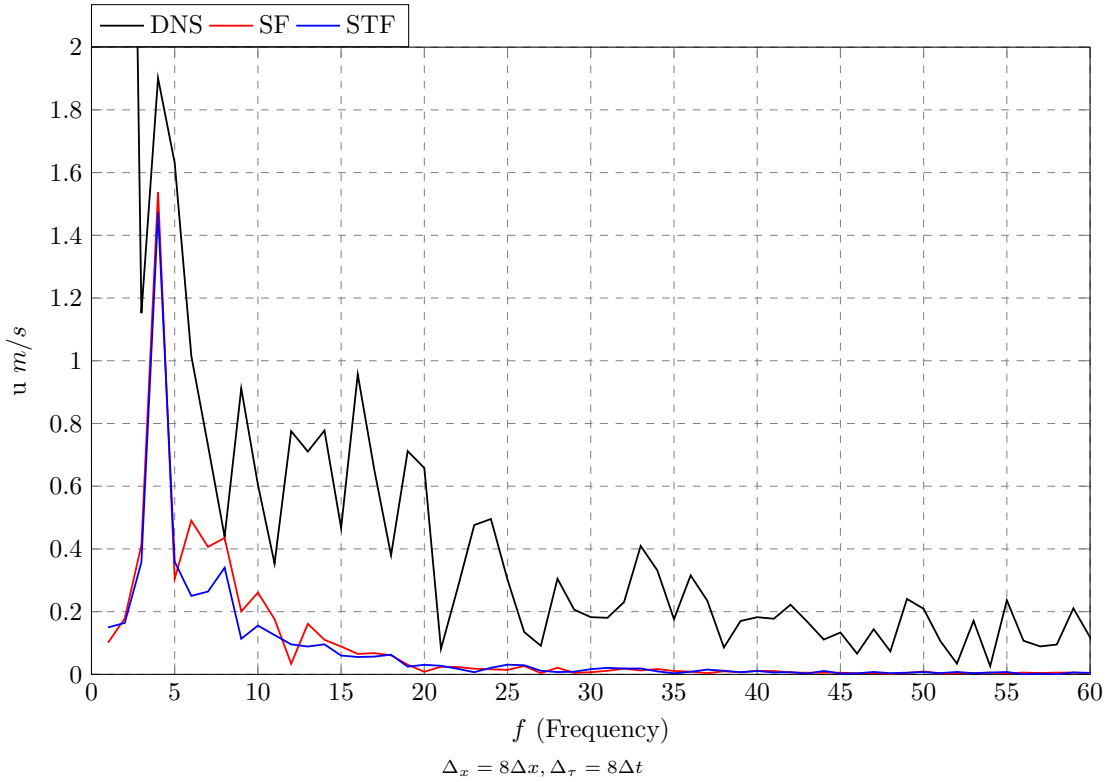


Figure 11: Comparison of frequencies from FFT of solutions using different filter sizes

As can be seen from Figure 8, the spatially-filtered and spatially-temporally-filtered solutions do not vary nearly as much from one another as they do from the "DNS" solution. As shown in Figure 9, the filter widths have a significant affect on the resulting wavenumber distributions (as would be expected). The filtering methods still show relatively little discernible difference in these figures. However, Figure 10 presents the difference between the solutions obtained with the filtered equations and the "DNS" solution. The differences are normalized by the "DNS" solution. As a result, these figures should be interpreted such that a value of zero is the highest accuracy, while larger values correspond to larger deviations of the filtered solutions from the "DNS" solution. In these particular cases, the low wavenumbers are of particular interest due to the fact that these are the wavenumbers that should be resolved with the filters. The case with the filter widths given by $\Delta_x = 2\Delta x$ and $\Delta_\tau = 2\Delta t$ shows little difference between the two filtering methods at low wavenumber. Since the filter widths are relatively small, the solutions from the two filtering methods are expected to be similar to one another and to what could be obtained without filtering at all on the course grid. However, as the filter width increases, the difference between the two methods is expected to increase, as it does in the second half of Figure 10. Furthermore, it is seen that, with filter widths of $\Delta_x = 8\Delta x$ and $\Delta_\tau = 8\Delta t$, the spatially-temporally filtered equation solution results in a wavenumber distribution closer to that of the "DNS" solution. This improvement in solution quality, while slight, encourages further study of the impact of filter sizes on the resulting solution quality.

The frequency data obtained from the simulations performed within this study is presented in Figure 11. It is apparent that, for smaller filter sizes, the frequency spectrum does not differ significantly between the two filtering methods. When larger filter sizes are used, the frequency spectrum of the spatially-temporally filtered equation is distinctly smoothed as compared with the frequency resulting from the spatially filtered equation. This smoothing provides a potential mechanism for greater control of aliasing error. Further studies will examine the quantitative quality of the solutions through comparison of the statistical information contained within the solutions.

## VI. Methodology for the Verification of the FAST LES Approach

Following the general guideline suggested by Dakhoul,[8] we have laid out the methodology for the verification procedure as follows. Note that the implementation of the methodology is left for a future follow-up study.

1. Obtain an "exact" solution of the original model equations on a fine grid that warrant a direct numerical simulation.
2. Filter the "exact" solution to get the large-scale components and compare it to the solution computed by the FAST and the spatial-only filtering approaches on a coarse grid that is coarsened sufficiently from the fine grid.
3. Examine the quantities such as the mean, variance, skewness, and kurtosis of the spatial distributions and their time histories, along with the energy spectrum and frequency spectra.
4. Compare the performance of the two SFS models.

## VII. Concluding Remarks and Future Work

In conclusion, the derivation of the FAST filtering framework is presented in this paper and is developed in such a manner that it can be easily applied to governing equations of compressible flows. The mathematical terms arising from application of the filter to nonlinear terms in governing equations is also explored in such a way that potentially new methods of SFS modeling are identified. The terms are developed in only a limited manner within this paper, but future research will focus on pushing these concepts further. In addition to the results from mathematical derivation, the simulations performed within the present study show the stability of the FAST filtering framework applied to the viscous Burgers' equation. These stability analysis results provide confidence that the stability of the FAST filtering framework is comparable with and even superior to the stability of the spatially-filtered framework. The simulations performed following the stability analysis demonstrate the variation among the solutions resulting from the unfiltered and filtered equations. It is seen that the spatially-temporally filtered equation shows an improved solution among all of the methods explored.

An immediate future research interest will be to refine and implement the methodology for the verification of the FAST LES approach through thorough analysis to demonstrate its validity. A second research interest of high priority will be the analysis of the commutation error associated with application of the spatial-temporal filter to spatial and temporal boundaries. This research will provide the basis of justification for the application of a symmetric, acausal filter to a finite, bounded, space-time domain. Additionally, study of the modification of the closure terms and the resulting solution quality will have a high priority. Investigations of the numerical and analytical weights of the higher order filter terms will also be performed in future work. Finally, the FAST filtering framework will be applied to the compressible Navier-Stokes equations and tested in future studies.

## A. Appendix A

Explicitly stating every filtering operation, we have the following form

$$\overline{\overline{\phi_i}\overline{\phi_j}} = \int_{-\infty}^{\infty} G(\vec{x}-\vec{\xi},t-\tau)\left[\int_{-\infty}^{\infty} G(\vec{x}-\vec{\xi},t-\tau)\phi_i(\vec{\xi},\tau)\,\mathrm{d}\vec{\xi}\,\mathrm{d}\tau\right]\left[\int_{-\infty}^{\infty} G(\vec{x}-\vec{\xi},t-\tau)\phi_j(\vec{\xi},\tau)\,\mathrm{d}\vec{\xi}\,\mathrm{d}\tau\right]d\vec{\xi}d\tau\ . \quad (66)$$

In preparation to solve for just one of the inner integrals, a Taylor expansion of $\phi_i$ is given by

$$\begin{aligned}\phi_i(\vec{\xi},\tau) &= \phi_i(\vec{x}+(\vec{\xi}-\vec{x}),t+(\tau-t))\\ &= \phi_i(\vec{x},t)+(\tau-t)\frac{\partial\phi_i(\vec{x},t)}{\partial t}+\sum_{d=1}^{D}(\xi_d-x_d)\frac{\partial\phi_i(\vec{x},t)}{\partial x_d}\\ &+\frac{1}{2}\sum_{d,e=1}^{D}(\xi_d-x_d)(\xi_e-x_e)\frac{\partial^2\phi(\vec{x},t)}{\partial x_d\partial x_e}+\sum_{d=1}^{D}(\xi_d-x_d)(\tau-t)\frac{\partial^2\phi(\vec{x},t)}{\partial x_d\partial t}\\ &+\frac{1}{2}(\tau-t)^2\frac{\partial^2\phi(\vec{x},t)}{\partial t^2}+\text{H.O.T.}\end{aligned} \quad (67)$$

The substitution of the Taylor expansion of $\phi_i$ into the inner filtering operation results in

$$\overline{\phi_i} = \int_{-\infty}^{\infty} G(\vec{x}-\vec{\xi},t-\tau)\phi_i\,\mathrm{d}\vec{\xi}\,\mathrm{d}\tau = \phi_i(\vec{x},t)+\frac{\Delta_\tau^2}{4\gamma}\frac{\partial^2\phi_i(\vec{x},t)}{\partial t^2}+\sum_{d=1}^{D}\frac{\Delta_d^2}{4\gamma}\frac{\partial^2\phi_i(\vec{x},t)}{\partial x_d^2}+\text{H.O.T.} \quad (68)$$

Furthermore, substituting this expression into $\overline{\phi_i}\overline{\phi_j}$ results in

$$\begin{aligned}\overline{\phi_i}\overline{\phi_j}(\vec{x},t) &= \phi_i\phi_j(\vec{x},t)+\frac{\Delta_\tau^2}{4\gamma}\phi_i(\vec{x},t)\frac{\partial^2\phi_j(\vec{x},t)}{\partial t^2}+\sum_{d=1}^{D}\frac{\Delta_d^2}{4\gamma}\phi_i(\vec{x},t)\frac{\partial^2\phi_j(\vec{x},t)}{\partial x_d^2}\\ &+\frac{\Delta_\tau^2}{4\gamma}\phi_j(\vec{x},t)\frac{\partial^2\phi_i(\vec{x},t)}{\partial t^2}+\sum_{d=1}^{D}\frac{\Delta_d^2}{4\gamma}\phi_j(\vec{x},t)\frac{\partial^2\phi_i(\vec{x},t)}{\partial x_d^2}\\ &+\left(\frac{\Delta_\tau^2}{4\gamma}\frac{\partial^2\phi_i(\vec{x},t)}{\partial t^2}\right)\left(\frac{\Delta_\tau^2}{4\gamma}\frac{\partial^2\phi_j(\vec{x},t)}{\partial t^2}\right)+\left(\sum_{d=1}^{D}\frac{\Delta_d^2}{4\gamma}\frac{\partial^2\phi_i(\vec{x},t)}{\partial x_d^2}\right)\left(\sum_{d=1}^{D}\frac{\Delta_d^2}{4\gamma}\frac{\partial^2\phi_j(\vec{x},t)}{\partial x_d^2}\right)\\ &+2\left(\frac{\Delta_\tau^2}{4\gamma}\frac{\partial^2\phi_i(\vec{x},t)}{\partial t^2}\right)\left(\sum_{d=1}^{D}\frac{\Delta_d^2}{4\gamma}\frac{\partial^2\phi_j(\vec{x},t)}{\partial x_d^2}\right)+\text{H.O.T.}\end{aligned} \quad (69)$$

Considering the form of Taylor expansions, it can be demonstrated that a finite expansion of $\phi_i\phi_j$ will contain fewer terms than the multiplication of the finite expansions of $\phi_i$ and $\phi_j$ (where the expansions in each of the three cases are truncated at the same order of derivatives). It can be shown that for a Taylor expansion of $\phi_i\phi_j$ with derivatives of order $n$, the derivatives can be simplified (by the chain rule of differentiation) to the general form

$$\frac{\partial^n\phi_i\phi_j}{\partial x_d^n} = \sum\frac{\partial^m\phi_i}{\partial x_d^m}\frac{\partial^p\phi_j}{\partial x_d^p}\ , \quad (70)$$

where $m+p \leq n$, and the coefficients and summation indices are left out of the summation. Upon extending the Taylor expansion of $\phi_i\phi_j$ to higher derivatives, it can be found that the multiplication of the expansions of $\phi_i$ and $\phi_j$ contains all of the terms present in the expansion of $\phi_i\phi_j$ and that the terms that do not follow $m+p \leq n$ in the multiplication of the individual Taylor expansions are present in the higher order derivatives of $\phi_i\phi_j$. Therefore, these terms can be removed from Eq. (69) in order to obtain the form

$$\begin{aligned}\overline{\phi}_i\overline{\phi}_j(\vec{x},t) = \phi_i\phi_j(\vec{x},t) &+ \frac{\Delta_\tau^2}{4\gamma}\phi_i(\vec{x},t)\frac{\partial^2\phi_j(\vec{x},t)}{\partial t^2} + \sum_{d=1}^{D}\frac{\Delta_d^2}{4\gamma}\phi_i(\vec{x},t)\frac{\partial^2\phi_j(\vec{x},t)}{\partial x_d^2} \\ &+ \frac{\Delta_\tau^2}{4\gamma}\phi_j(\vec{x},t)\frac{\partial^2\phi_i(\vec{x},t)}{\partial t^2} + \sum_{d=1}^{D}\frac{\Delta_d^2}{4\gamma}\phi_j(\vec{x},t)\frac{\partial^2\phi_i(\vec{x},t)}{\partial x_d^2} + \text{H.O.T.}\end{aligned} \tag{71}$$

Now, Eq. (66) can be carried out as

$$\overline{\overline{\phi_i\overline{\phi}_j}} = \int_{-\infty}^{\infty} G(\vec{x}-\vec{\xi},t-\tau)\overline{\phi}_i\overline{\phi}_j(\vec{\xi},\tau)\,\mathrm{d}\vec{\xi}\,\mathrm{d}\tau \ , \tag{72}$$

with the use of Eq. (71)

$$\begin{aligned}\overline{\overline{\phi}_i\overline{\phi}_j}(\vec{x},t) = \phi_i\phi_j(\vec{x},t) &+ \frac{\Delta_\tau^2}{4\gamma}\frac{\partial^2\phi_i\phi_j}{\partial t^2} + \sum_{d=1}^{D}\left(\frac{\Delta_d^2}{4\gamma}\right)\frac{\partial^2\phi_i\phi_j}{\partial x_d^2} \\ &+ \frac{\Delta_\tau^2}{4\gamma}\phi_i(\vec{x},t)\frac{\partial^2\phi_j(\vec{x},t)}{\partial t^2} + \sum_{d=1}^{D}\frac{\Delta_d^2}{4\gamma}\phi_i(\vec{x},t)\frac{\partial^2\phi_j(\vec{x},t)}{\partial x_d^2} \\ &+ \frac{\Delta_\tau^2}{4\gamma}\phi_j(\vec{x},t)\frac{\partial^2\phi_i(\vec{x},t)}{\partial t^2} + \sum_{d=1}^{D}\frac{\Delta_d^2}{4\gamma}\phi_j(\vec{x},t)\frac{\partial^2\phi_i(\vec{x},t)}{\partial x_d^2} + \text{H.O.T.}\end{aligned} \tag{73}$$

where all of the individual filter applications were truncated such that only second-order derivatives remained. As a result, the approximation of the filtering of $\phi_i\phi_j$ is maintained to second-order derivatives while the approximations of the filtering of all the higher terms were only maintained to a first order approximation (zeroth-order derivatives). In comparison to Eq. (16), Eq. (73) is a different expression to approximate $\overline{\overline{\phi}_i\overline{\phi}_j}$. It is worth mentioning that a formulation of this form could be of interest in the future for determining the deviation of the filtered quantity from the original unfiltered quantity.

## References


[1]Subcommittee, A. S. C. A. C., "The opportunities and challenges of exascale computing," Tech. rep., DOE, 2010.

[2]Yang, Z., "Large-eddy simulation: Past, present and the future," *Chinese Journal of Aeronautics*, Vol. 28(1), 2015, pp. 11–24.

[3]Dakhoul, Y. and Bedford, K., "Improved averaging method for turbulent flow simulation. Part I: Theoretical development and application to Burgers transport equation," *International Journal for Numerical Methods in Fluids 6.2*, 1986, pp. 49–64.

[4]Dakhoul, Y. and Bedford, K., "Improved averaging method for turbulent flow simulation. Part II: Calculations and verification," *International Journal for Numerical Methods in Fluids 6.2*, 1986, pp. 65–82.

[5]Pruett, C., "Eulerian time-domain filtering for spatial large-eddy simulation," *AIAA J.*, Vol. 38, 2000, pp. 1634–1642.

[6]Carati, D. and Wray, A., "Time filtering in large-eddy simulations," *Proceedings for the Summer Program*, Center for Turbulence Research, 2000, pp. 263–270.

[7]Garnier, E., Adams, N., and Sagaut, P., *Large Eddy Simulation for Compressible Flows*, Springer, 2009.

[8]Dakhoul, Y. M., *Improved Averaging Method for Turbulent Flow Simulations*, Ph.D. thesis, The Ohio State University, 1983.

[9]Smagorinsky, J., "General circulation experiments with the primitive equation," *Mon. Wea. Rev.*, Vol. 91, 1963, pp. 99–152.

[10]Sagaut, P., *Large Eddy Simulation for Incompressible Flows: An Introduction*, Springer-Verlag, 3rd ed., 1998.

[11]Wu, X. and Moin, P., "A direct numerical simulation study on the mean velocity characteristics in turbulent pipe flow," *J. Fluid Mech.*, Vol. 608, 2008, pp. 81–112.

[12]Wu, X., Moin, P., Wallace, J. M., Skarda, J., Lozano-Duran, A., and Hickey, J.-P., "Transitional-Turbulent Spots and Turbulent-Turbulent Spots in Boundary Layers," *Proceedings of National Academy of Sciences*, 2017.

[13]Guzik, S. M., Gao, X., Owen, L. D., McCorquodale, P., and Colella, P., "A Freestream-Preserving Fourth-Order Finite-Volume Method in Mapped Coordinates with Adaptive-Mesh Refinement," *Comput. Fluids*, Vol. 123, 2015, pp. 202–217.

[14]Gao, X., Guzik, S. M. J., and Colella, P., "Fourth Order Boundary Treatment for Viscous Fluxes on Cartesian Grid Finite-Volume Methods," AIAA 2014-1277, 52nd AIAA Aerospace Sciences Meeting, 2014.